國立交通大學

運輸科技與管理學系

碩士論文

含移動方程巨觀動態車流模式之建立

Macroscopic Dynamic Traffic Flow Model with Mobility Function

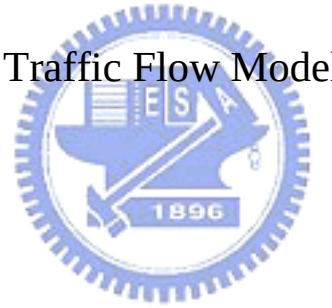

研 究 生：林杜寰

指導教授：卓訓榮　教授

中 華 民 國 九 十 四 年 六 月

含移動方程巨觀動態車流模式之建立

學生：林杜寰　　指導教授:卓訓榮

國立交通大學運輸科技與管理學系碩士班

摘　　要

本研究目地在發展一套新的動態巨觀車流模式，並且導入交通場與機動力的概念構建此模式。在本研究中，交通場又可分為外場與內場，前者收道路外在環境之影響，後者則跟相鄰兩車之間的互動有關，交通場的大小決定了車輛在道路上的加減速行為。機動力在本研究中代表不同駕駛習慣之參數，它將扮演一個重要的因子，且所有車輛行為都將受其影響，不管是交通場的選擇門檻或者是加減速與變換車道的行為。為了讓所有模式中的變數與參數有其物理意義，本研究在構建巨觀模式之前，先行根據交通場與機動力的概念設計一微觀車流模式，並且藉由本研究設計之模擬器校估此微觀模式中各參數以及變數之間的關係，最後再將其推導成巨觀模式。我們應用蒙地卡羅法決定模擬時車輛的速度變化。除此之外，本研究處理多車道車輛行為時加入一車輛慣性之變數，此變數可以描述駕駛者在不同車道間變換所產生的衝擊，包括對他自己以及其他駕駛的影響。

Macroscopic Dynamic Traffic Flow Model with Mobility Function

student：Du-Hwan Lin Advisors：Dr. Hsun-Jung Cho

Department of Transportation Technology and Management
National Chiao Tung University

ABSTRACT

The purpose of this research is to develop a new dynamic macroscopic model. In this research, we introduce the traffic fields and mobility into this new model. The traffic field is subdivided into external field and internal field, the external field is caused by the external conditions in the roads and the internal field is caused by the interactions between the adjacent cars. We assume that all cars move fast or slowly according to the magnitude of traffic field. Mobility is a key factor to affect the behaviors of vehicles and the thresholds of traffic fields. We design a microscopic model first and calibrate the model by the result of our simulator. The simulator is designed based on CA model. We define the magnitude of acceleration and deceleration in the simulator according to Monte Carlo computing technique. After that, we derive the macroscopic model from the microscopic one. It is the reason that every variables and parameters in this research are meaningful. Besides, we define a new variable, Driver's inertia, to describe the shock caused by the lane-changing behaviors.

誌　　謝

終於，一切的辛苦有了些許收穫，這兩年雖然過的艱辛，還好有陪我一同走過的朋友、貴人及老師，是你們的包容傾聽、支持與開導，讓我在遇到挫折對一切感到無力的時後候，不會感到寂莫無助失去方向，是你們與我一同撐過那些昏天黑地團團轉的生活，讓日子裡除了辛苦還添增了不能缺少的快樂，用我最真誠的心意－謝謝你們。

以此獻給我親愛的朋友及摯愛的家人

Contents

List of Figures

List of Tables

CHAPTER 1

Introduction

Intelligent transportation systems (ITS) are the systems that employ advanced information and communication technologies to the operations of existing transportation systems in order to ensure traffic safety, improve traffic congestion, and decrease environmental impacts. For the purpose of ITS applications, a real-time prediction is needed. Managing traffic real-time in congested road or networks requires a clear understanding of traffic flow operations. For this purpose, during the past fifty years, there were a wide range of traffic flow theories and models, which were developed to answer these research questions.

1.1 Research Motivation and Objection

Traffic flow models are classified into microscopic and macroscopic models. The former model can use to describe slight movements of vehicles and to correct the model itself according to the behaviors of drivers. But using microscopic models wastes much time to simulate all traces of vehicles. That is the reason why simulator can't be used as real-time prediction, especially in large scale network. Even though the development of computer decreases the simulation time in recent years, we still can't use microscopic models to do real-time prediction. Macroscopic models based on fluid dynamic equations have been proposed by a large number of groups (ref. Lighthill, Whitham [27], and Payne [43]). However, there is a huger controversy over the applicability of traffic flow and the validity in these models.

There are many immeasurable parameters and variables in the past macroscopic models such as relaxation time. Though most of the models are focused on no-signal and one-dimension traffic flow, there are some problems in the backward traffic flow. Also, the behaviors between adjacent cars are neglected in these models. Even though the purpose of many new macroscopic models was to overcome most drawbacks of old ones in recent years, it complicates the models at the same time. We can't find the answer of the complicated models analytically unless using some numerical methods. Finite difference method is the most famous way to solve these models, but it reduces the efficiency of simulator especially for solving speed. Another problem of complicated models occurs because these models introduce many assumptions from gas kinetic field. The variables and parameters of gas kinetic field can't be explained well in traffic field.

We define a new variable called traffic field in this research. The traffic field is subdivided into external field and internal field, the former field is caused by the external conditions in roads and the latter field is caused by the interactions between adjacent cars. We assume that all cars move fast or slowly according to the magnitude of traffic field and derive a new macroscopic model from a microscopic one. The method ensures physic meanings of all variables and parameters. Finally, we define a variable called mobility to represents the behaviors of different drivers.

1.2 Research Scope and Procedure

In the evolution of transportation, dynamic traffic management seems to be a feasible way to relieve congestion. According to the types of field data and applications, dynamic traffic researches can be classified into three categories, that is the dynamic origin/destination (dynamic O/D) estimation, the dynamic traffic flow theory, and the dynamic traffic assignment. A complete dynamic management system includes three kernels, and the relation between them is illustrated in Figure 1.1. Since whole procedure is a cycle, each part can be an initial step. If the dynamic travel cost (or travel time) of each path in the network is known, the dynamic origin/destination table will be generated from the dynamic O/D model. If the dynamic travel cost (or travel time) of each link and the dynamic O/D table in the network are known, the path flow will be obtained by the dynamic assignment model. If flow on each path is known, travel time and dynamic link flow are obtained from dynamic traffic flow model.

This research derives a traffic flow model to predict travel time. The scope of the research is showed as the dotted frame in Fig1-1.

Because we define the traffic fields and the mobility in this research to derive a macroscopic model, we explain the meanings of them first. After that, we discuss the movements of cars caused by traffic fields and derive a model according to the movements. Finally, we design a simulator to prove our assumptions and calibrate all parameters in the models. The flowchart of this research is illustrated in Fig 1-2.

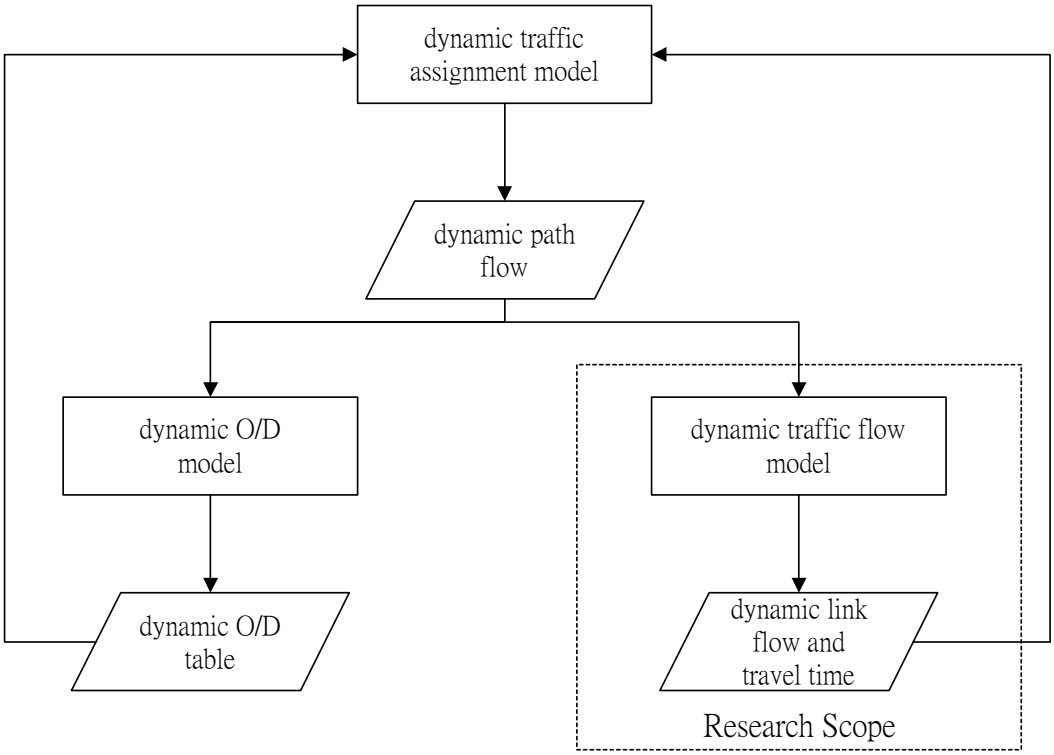

Figure 1-1 The architecture of dynamic traffic management system

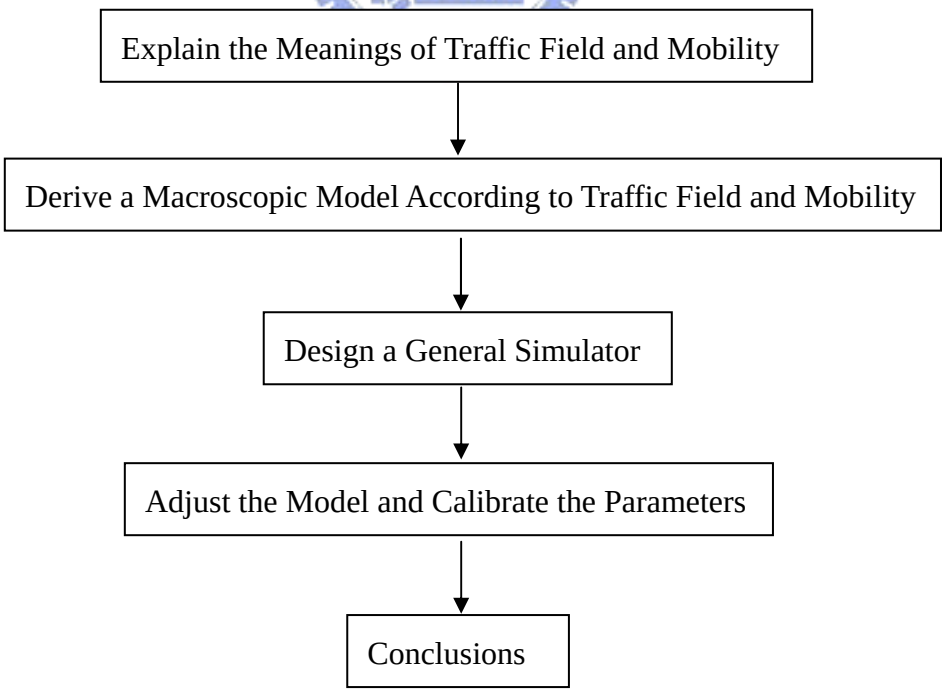

Figure 1-2 The flowchart of this research

CHAPTER 2
Literature Review

To develop a macroscopic traffic flow model, we derive it from a microscopic one in this research. For the purpose, we start with past microscopic and macroscopic models in this chapter. For developing a simulator based on CA models, they would be reviewed briefly later. A brief summary of traffic flow model would be described in the end of this chapter.

2.1 Microscopic Traffic Flow Models

The movements of all vehicles in the road are described in microscopic models more completely than in macroscopic ones. We could adjust all behaviors slightly base on microscopic models. We review some important microscopic traffic flow models from 1950 and focus on car-following behaviors to be the basis of simulator in this section.

2.1.1 Stimulus – Reaction Function

Microscopic models are designed based on car-following theory which is derived from Reuschel(1950)[47] and Pipes(1953)[46]. Gazis, Herman, and Potts[15] explained the car-following theory completely in 1959. They assumed all cars move in alignment and keep a safe distance from each other to avoid incidents. For keeping a safe distance, the velocity of following car should be adjusted according to the leading car. We derive Eq. (2.1) from stimulus-reaction function:

$$M\ddot{x}_{n+1}(t) = \lambda\left(\dot{x}_n - \dot{x}_{n+1}\right)_{t-\Delta} \tag{2.1}$$

$x_n(t)$ denotes the location of nth car, M denotes the weight of car, λ denotes a sensitive parameter, and Δ denotes the reaction time. If divers situate in equilibrium traffic flow, we can combine M with λ to be a sensitive term. In steady state, if the leading car changes its' velocity to be u, the following car will also move with velocity u. We let the distance between adjacent cars to be $h_n = x_n - x_{n+1}$ and obtain $h - h_0 = M(u - u_0)/\lambda$ from the initial condition. Because the distance is the reciprocal of density, we can derive Eq. (2.2) from above-mentioned equations:

$$k^{-1} - k_0^{-1} = M(u - u_0)/\lambda \quad \text{or} \quad u = u_0 + (\lambda / M)(k^{-1} - k_j^{-1}) \tag{2-2}$$

k_j denotes the jam density. Except the discussion of basic theory, Gazis[16] also derived the sensitive term showed as Eq. (2.3):

$$\lambda = \alpha \times \frac{x_{n+1}^m(t)}{(\dot{x}_n(t) - \dot{x}_{n+1}(t))^l} \tag{2.3}$$

α denotes the constant, m denotes the power parameter to response to the relation between the reaction time and the sensitive term, and l denotes the power parameter to response to the relation between the gap and the sensitive term.

2.1.2 Four Restrictive Functions

The purpose of these functions is keeping a minimum safe distance between two adjacent cars. If the following car maintains a safe distance from the leading car, it can move and brake safely. All restrictions are described as follows:

A. Spacing Restriction

The following car must keep a safe distance for the purpose of safety:

$$S = P + K_1 V_F + K_2 \frac{V_F^2 - V_L^2}{2D} \times C \tag{2.4}$$

In Eq. (2.4):

S ：Safe distance
P ：Effective length of the leading car
K_1 ：Reaction time of the following car
K_2 ：Constant，1m/s in MKS
V_F ：Velocity of the following car
V_L ：Velocity of the leading car
D ：Average deceleration of the following car
C ：Constant，when $V_F > V_L$, C=1 , otherwise, C=0

B. Acceleration Restriction

The maximum distance that general car can reach in a unit time.

C. Stopping Restriction

The distance that cars can reach in a unit time when they meet a red light or some other conditions to induce them to decelerate

D. Turning Restriction

When drivers make a turn and receive a centrifugal force at the same time. They

must decelerate to avoid losing the control of car.

Above-mentioned restrictions are the limit of the maximum distance that general cars can move in a unit time.

2.1.3 PITT Model

PITT is a FRESIM model in CORSIM developed by FHEA. Its' theory is keeping a space headway:

$$H = L_L + k \times V_F + 10 + b \times k \times (V_L - V_F) \qquad (2.5)$$

In Eq. (2.5):

H ：Space headway(ft)
V_F ：Velocity of the following car
V_L ：Velocity of the leading car
L_L ：Length of the leading car
k ：Sensitivity of the driver
b ：Constant, when V_L=V_F≤ 10,C=0.1, otherwise, C=0

For keeping above-mentioned gap, the acceleration of the leading car is:

$$A_F = \frac{2\left[X_L - X_F^i - L - 10 - V_F^i \times (k \times T) - b \times k \times (V_L - V_F^i)^2\right]}{\left(T^2 + 2 \times k \times T\right)} \qquad (2.6)$$

In Eq. (2.6):

A_F ：Acceleration of the following car
X_L ：Location of the leading car
X_F^i ：Original location of the following car
V_F^i ：Original velocity of the following car
T ：Scanning gap(sec)

, The velocity of the following car is $V_F = V_F^i + A_F \times (T - c)$ when we take the reaction time into account. To avoid traffic accident, PITT designs three constricted functions [25].

2.1.4 Behavioral Threshold Model

There are two unreasonable assumptions in stimulus-reaction function:

1. There are interactions between adjacent cars no matter how long the distance between them is.
2. When relative velocity is constant, the velocity of the following car is

constant.

The following car, in fact, will accelerate when the distance or the relative velocity between the leading car and itself is large. If the distance between two cars is large enough, the movements of following car would be unrestricted. The above-mentioned behaviors represent a special car-following phenomenon showed as Fig 2-1[26]:

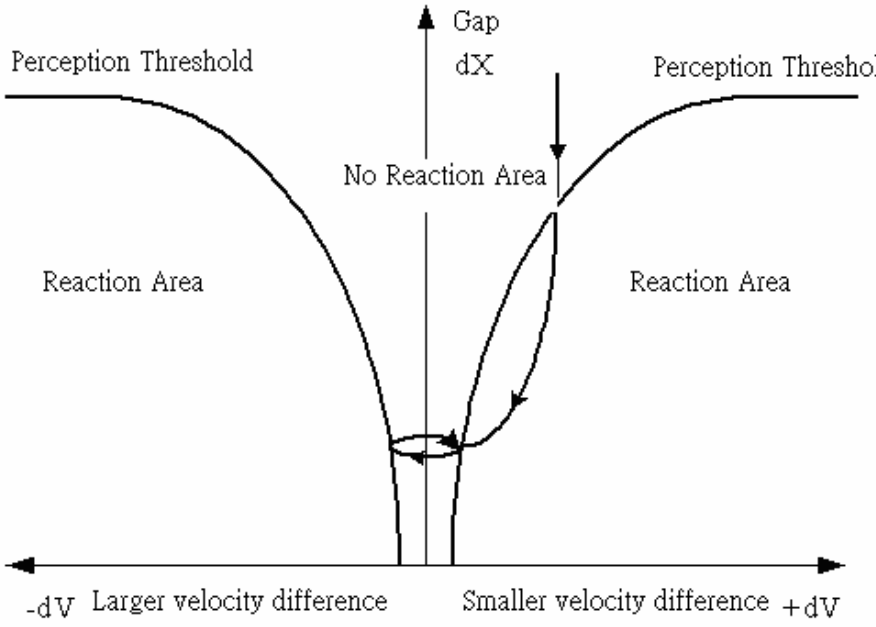

Figure 2-1 Relative movement between leading and following cars

Wiwdemann[53] introduced the Psycho-Physical Spacing Model into microscopic simulator and designed the INTAC Model to be the Behavioral Threshold Model. He assumed that cars move in single lane and have no lane-changing behaviors. In Behavioral Threshold Model, traffic flow conditions are classified into three reaction areas: (1) Perceived Reaction (2) Unconscious Reaction (3) No Reaction. Above-mentioned phenomenon is showed in Fig. 2.2:

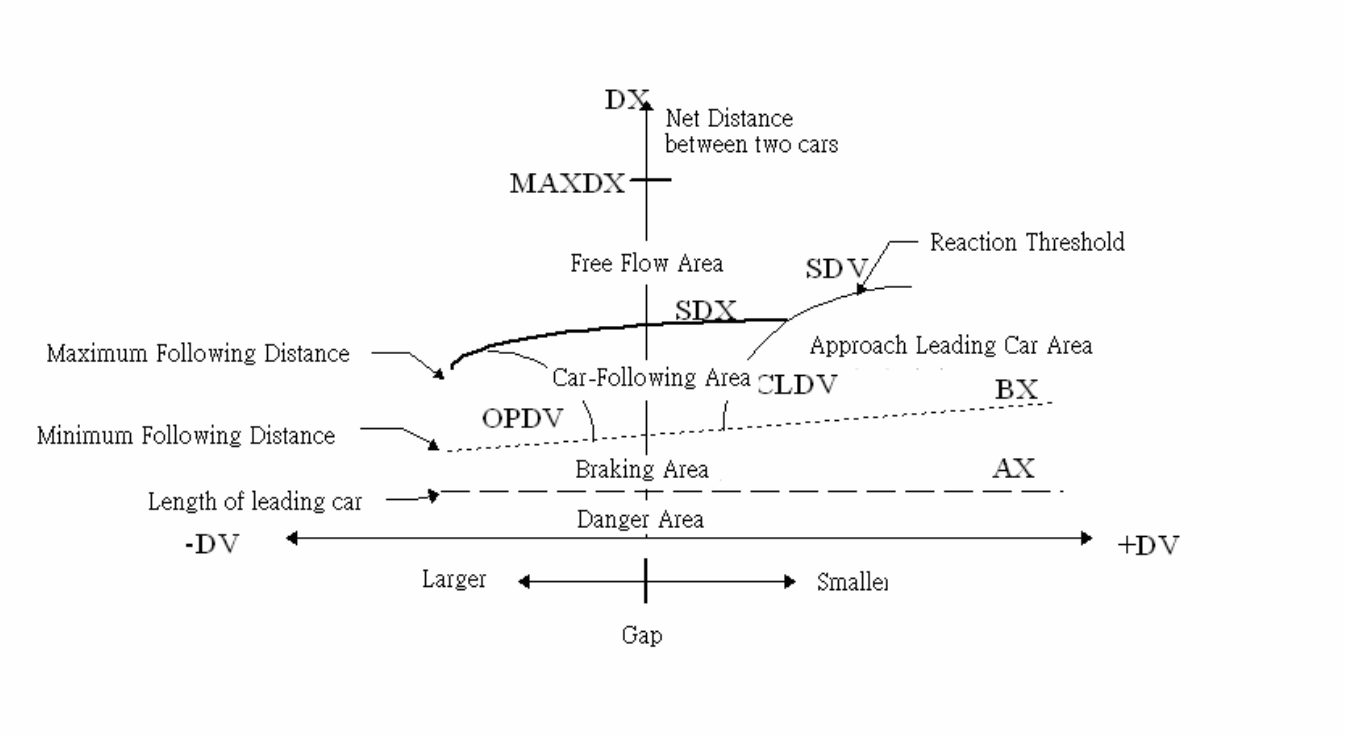

Figure 2-2 Relation of behavioral threshold model

The meaning of each threshold is:

A. AX: Desire distance between two cars when the following car is static.

B. BX: When the velocity difference between two cars is small, it is a minimum distance that following car desire.

C. SDV: It is the velocity difference perceived threshold of following car when the distance between two cars is large.

D. SDX: The range of SDX is 1.5~2.5 according to the difference between different drivers.

E. CLDV: It is a velocity threshold when the gap between two cars is small and the velocity of the following car is larger than the leading one. It is calculated from SDV and random factors.

F. OPDV: It is a velocity threshold when the gap between two cars is small and the velocity of the following car is smaller than the leading one.

2.1.5 CARSIM

CARSIM(CAR-Following Simulation Model) was developed by Benekohal[4]. Vehicles are classified into five classes in CARSIM showed as follows:

A1: General driving behaviors with the velocity which is under the maximum velocity

A2: General driving behaviors with the velocity which is equal to maximum velocity

A3: The vehicles which are starting to move

A4: The driving behaviors with enough gap:

$$X_L - \left(X_F + V_F(DT) + 0.5(A4)(DT)^2\right) \geq L_L + K \tag{2.7}$$

In Eq. (2.7)：

X_L ：Location of the leading car
X_F ：Location of the following car
L_L ：Length of the leading car
K ：Buffer distance between two cars
DT ：Scanning gap(sec)
$A4$ ：The acceleration and deceleration in this condition

A5: The driving behaviors which limit to safe constraints

A5 is a combination of A4 and some safe constraints showed as follows:

$$X_L - \left(X_F + V_F(DT) + 0.5(A5)(DT)^2\right) - L_L - K \geq \text{maximum of} \begin{vmatrix} [V_F + (A5)(DT)](BRT), \\ \left[V_F + (A5)(DT)\right](BRT) + \dfrac{[V_F + (A5)(DT)]^2}{2(MX.F)} - \dfrac{X_L{}^2}{2(MX.L)} \end{vmatrix} \tag{2.8}$$

In Eq. (2.8)：

BRT ：Reaction time to brake safely
V_L ：Velocity of the leading car in the end of time step
$MX.F$ ：Maximum deceleration of the following car
$MX.L$ ：Maximum deceleration of the leading car
$A5$ ：The acceleration and deceleration in this condition

2.2 Static Macroscopic Traffic Flow Models

Velocity, density, and flow are three important factors in macroscopic

models. Their relation showed as Eq. (2.9):

$$q = ku \tag{2.9}$$

Greenshield [20](1934) and Olcott [41](1955) showed that an approximate linear relationship between speed and density of traffic exists, whereby, as the average speeds of vehicles increase, the density of the traffic stream decreases. Greenberg [19](1959) suggested that an equation describing the steady state relation between Q and k, or between u, the velocity of the stream, and k could be derived by assuming a particular equation of state for the fluid. Characteristics and distributions of hourly volumes and average speed are discussed by Vaughan [52](1970) , Gazis, and Knapp [14](1971) , Makigami, Newell, and Rothery [28](1971). Other research results of the static macroscopic traffic flow model are summarized in Table 2-1 and Table 2-2.

Table 2-1 Table of single-regime models

Single-regime models	Equations
Greenshields model (1934)	$u = u_f\left(1-\frac{k}{k_j}\right)$
Greenberg model (1959)	$u = u_0 \ln\left(\frac{k_j}{k}\right)$
Underwood model (1961)	$u = u_f e^{-k/k_0}$
Northwestern's model (1967)	$u = u_f e^{-1/2(k/k_o)^2}$
Drew model (1968)	$u = u_f\left[1-\left(\frac{k}{k_j}\right)^{(n+1)/2}\right]$
Pipes-Munjal model (1967)	$u = u_f\left[1-\left(\frac{k}{k_j}\right)^{n}\right]$
	u_f ：free flow speed k_j ：congested density u_o ：critical speed k_o ：critical density

reference: May(1990)

Table 2-2 Table of multi-regime models

Multiregime models	Free-flow regime	Transitional-flow regime	Congested-flow regime
Edie model (1961)	$u = u_f e^{-k/k_0}$ $(k \le k_o)$	—	$u = u_0 \ln\left(\frac{k_j}{k}\right)$ $(k \ge k_o)$
Two-regime linear model (1967)	$u = u_f\left(1-\frac{k}{k_j}\right)$ $(k \le k_1)$	—	$u = u_f\left(1-\frac{k}{k_j}\right)$ $(k \ge k_1)$
Modified Greenberg model (1967)	constant speed $(k \le k_2)$	—	$u = u_0 \ln\left(\frac{k_j}{k}\right)$ $(k \ge k_2)$
Three-regime linear model (1967)	$u = u_f\left(1-\frac{k}{k_j}\right)$ $(k \le k_3)$	$u = u_f\left(1-\frac{k}{k_j}\right)$ $(k_4 \le k \le k_3)$	$u = u_f\left(1-\frac{k}{k_j}\right)$ $(k \ge k_4)$
	k_i ：specified traffic density ，i=1.2.3.4		

reference: May[29](1990)

2.3 CA Models

A more recent addition to the development of vehicular traffic flow theory is cellular automation (CA) or particle hopping method. Although CA is first proposed long ago (Gerlough)[17](1956), CA has begun to receive wide attention of statistical physics community only after the simple formulation by Nagel and Schreckemberg [37](1992). In CA, a road is represented as a string of cells, which are either empty or occupied by exactly one vehicle. Movement takes place by hopping between cells.

CA is defined as follows. Each vehicle can have an integer velocity between 0 and $u_{\max}$. The complete configuration at time step *t* is stored, and the configuration at time step *t+2* is computed from that, i.e., using a parallel or synchronous update. All vehicles execute in parallel the following steps:

(i) Let *g* (gap) equal the number of empty sites ahead.

(ii) If *u*>*g* (too fast), then slow down to *u*=*g* (rule 1); otherwise if u<g (enough

headway) and $u < u_{maz}$, then accelerate by one $u=u+1$ (rule 2).

(iii) Randomization: If after the above steps the velocity is larger than zero (u>0), then, with probability p, reduce u by one (rule 3).

(iv) Vehicle propagation: Each vehicle moves u sites ahead (rule 4).

Pesheva et al. [44](1997) proposed a CA (particle hopping) to describe 1D traffic flow under a bottleneck situation. Then Rickert [50](1996) extended CA to a two lane traffic condition. Furthermore, Chowdhury [5](1997) a two-lane traffic with two kinds of vehicles. CA also can be built as a control model. Hattori [22](1999) and Jin et al. [24](1999) applied CA to signalize intersection with periodic boundary condition. With respect to the capacity of the signalized intersection, Nagel [36](1996) and Nagatani [35](1996) considered the several different acceleration effects of vehicles in CA models.

Nagel [36](1996) compared the other models to CA and made some conclusions as follow:

(i) Robust computing: CA is known to be numerically robust especially in complex geometries.

(ii) University: Intuitively, a relatively simple microscopic model should be able to show the essential features of traffic jams. One might even speculate that the critical exponents of traffic jam formation are universal.

(iii) Towards minimal models: The present results show that close-up car-following behavior is not the most important aspect to traffic model. The important crucial aspect is to model deviations from the optimal (smooth) behavior and the ways in which they lead to jam formation. Another important aspect, which seems far from obvious, is the acceleration behavior, especially when there are other vehicles ahead, since it is the acceleration behavior that mostly determines the maximum flow out of a jam (which may be a simple traffic light).

(iv) Traffic dynamics: Fast running and easy to implement CA can be very useful in interpreting measurements.

(v) Microscopic simulation: CA is inherently microscopic, which allows one to add individual properties to each vehicle.

(vi) Stochastic and fluctuations: Last but not least, CA are stochastic in nature, thus producing different results when using different random seeds even

when starting from identical initial conditions. The traffic system is inherently stochastic and the variance of the outcomes is an important variable itself.

CA is a kind of microscopic models and inherits the advantages and disadvantages of them. Although its concept is posed many years ago, the physical models are presented recently. It is claimed that it has the potential to model and describe real problems well. However, in motorcycles and vehicles mixed traffic, motorcycles are not restricted in single lane. Their motion should be treated as two-dimensional behavior. As researches, which are proposed by car-following theory in Taiwan, the model may become very complicate and the behavior may not be easily modeled anymore. In addition, the more complicate CA induce much more robust numeric can be forecasted.

2.4 Dynamic Macroscopic Traffic Flow Models

Lighthill and Whitham [27](1955) and Richards [49](1956) are the first people that presented the macroscopic kinetic traffic flow model. The basic theory of their model is that traffic is conversed and that there exists a one-to-one relation between velocity and density. The LWR model can be viewed as a good and basic approximation. Mathematically, LWR model states that the density k and flow Q satisfy

$$\frac{\partial k(x,t)}{\partial t} + \nabla \cdot Q(x,t) = 0 \tag{2.10}$$

where t denotes time and x denotes position. Eq. (2.10) expresses the conservation of vehicles. In addition, Q, k and velocity u are assumed to satisfy $Q=ku(k)$. From these assumptions, Eq. (2.10) has the solution $k=F(x-ct)$, where F is an arbitrary function (the initial condition), c is the wave speed and $c = dQ/dk$. Eq. (2.10) implies that in homogeneities, such as changes in density of cars, propagate along a stream of cars with constant wave speed c with respect to a stationary observer.

The assumption of $u=u(k)$ is a steady state assumption of velocity, which means that velocity changes instantaneously as density changes. It is certainly not

valid in some traffic flow situations. To overcome the steady state assumption of velocity, Payne [43](1979) used a motion equation to obtain time variant speed.

$$\frac{\partial u}{\partial t}+u(\nabla\cdot u)=-\frac{1}{k}\nabla\cdot(P_e(k))+\frac{1}{\tau}(u_e(k)-u) \tag{2.11}$$

where $u_e(k)$ is an equilibrium speed-density relation and τ is the relaxation time. Parpageorgiou[42](1982) used Euler-like discrete Form which shows as Eq. (2.12) to improve the efficiency of Payne's models in computer.

$$\frac{\partial u}{\partial t}+uV\frac{\partial u}{\partial x}=\frac{1}{T}\{[u_e(k)-u]-\frac{v}{k+k}\frac{\partial k}{\partial x}\} \tag{2.12}$$

Michalopoulos, Yi, and Lyrintzis [34](1993) developed a semi-viscous model, which substitutes a viscosity term into Eq. (2.11), show as Eq. (2.13) and (2.14):

$$\frac{\partial u}{\partial t}+u\frac{\partial u}{\partial x}=\frac{1}{T(k)}\{[u_f(x)-u]-ak^b\frac{\partial k}{\partial x}\} \tag{2.13}$$

$$\frac{\partial u}{\partial t}+u\frac{\partial u}{\partial x}=-ak^b\frac{\partial k}{\partial x}+hk^p\frac{\partial^2 k}{\partial x^2} \tag{2.14}$$

Michalopoulos and Pisharody [31](1980) and Michalopoulos et al. [32](1980, 1981) also employed the LWR model and shock wave analysis to derive an isolated real time signal control. Del Castillo et al. [10](1994) proposed an expression for the reaction time of drivers as a function of traffic density in the PW model. Later, Del Castillo, and Benitez [12](1995a, 1995b) presented a functional form for the speed-density relationship. This functional form is made up of a nondimensional spacing the equivalent spacing and of a function, the generating function, whose argument is the equivalent spacing. This functional form is derived by means of two different arguments. The first argument is based on the set of properties that the volume-speed-density relationship should satisfy. The second one arises when applied to a dimensional analysis of a generic car-following model.

In addition to the LWR model, Baker [1](1981) and Daganzo [7](1994) brought up different dynamic macroscopic traffic flow models. Baker considered the continuity, jam-packed, diffusivity, and fluidity of the traffic flow. He used the speed as the main viewpoint, and introduced the concept of velocity field to construct velocity potential model. Moreover, Baker [2](1983) derived the hydrodynamic model of the traffic flow. The key point of the model still lay on the conditions of crowded

traffic flow and fleet diffusion. The model is a molecule dispersive equation which uses the end of the road as the boundary conditions of the free traffic flow. It is used to analyze the periodic traffic flow characteristics of signal intersections. It is as well as the Schrodinger equation in the quantum physics. Daganzo use the concept of cell propagation to construct the time-space variations of traffic flow of a single entrance/exit highway, concluding the formation, propagation and diffusion of fleet. The purpose of using cell propagation is to find the locations where the density changed, that is, the locations where the density is not continuous, just as the shock wave analysis does.

2.5 Summary

A useful dynamic model must support a correct data about flow and travel time. Obviously, we find some drawbacks in past literatures:

A. There is no relation between variables in static models.
B. Scholars usually introduce static model or experiential model into motion equation and neglect whether they have physic meanings.
C. There is lack of the descriptions of each factor in past motion equations.

We overcome above-mentioned drawbacks to design a new dynamic traffic models.

CHAPTER 3

Single Lane Traffic Flow Model

For describing the movements affected by vertical distance between cars, macroscopic models are usually designed as one-dimension models. These models also represent the effects caused by speed difference between leading and following cars. There are four sections in this chapter: (1)We explain the meanings of the traffic fields and mobility in first section and design a general microscopic model based on Newton's laws and some practical behaviors. (2)We describe the details of our simulator and the assumptions about moving behaviors of cars in second section. (3)We use the data of the simulator to verify the model designed in first section. (4)We derive a macroscopic model from microscopic one in latest section. The studies about muti-lane would be discussed in next chapter.

3.1 Traffic Fields and Mobility

We assume all cars would be affected by a external field according to Newton's laws in this research. The magnitude of field is based on all external factors such as gradient, number of lane, geometrical design, and so on. Moreover, there is a force between two adjacent cars which is defined as internal field in our study. It is the reason that car equivalent, and the distance and the speed difference between cars are the factors to affect the magnitude of internal field. We believe that the acceleration is affected by internal fields according to Newton's laws. It is the reason that we define the force to put cars moving in light traffic called external field and the extra-force in heavy traffic called internal field. So we define a total field showed as Eq. (3.1):

$$E_{\text{total}} = E_{\text{external}} + E_{\text{internal}} \qquad (3.1)$$

3.1.1 Internal Field

In last section, we describe the fields affected by distance between cars which are defined to be inverse proportion in Newton's laws. There are some problems in above assumption. For example, if two cars move closely, the following car would decelerate

based on Newton's laws. But we know that if cars move closely, the following driver would maintain his velocity to be the same as the leading car if he contains a safe distance. Another special example is that if two cars move apart a long distance but the leading car move much slower than the following one. The following car would decelerate even though the distance between them is large. Because of above-mentioned reasons, we determine the field not only affected by distance in this research.

We observe the practical behaviors to find that drivers make decisions to decelerate or accelerate according to the time that they would bump into the leading car if both two cars contain constant velocity. We define it to be the **probability of bump (POB)**. The internal fields and POB must be direct proportion by the definitions.

Before finding the correct relation between internal field and **POB**, we assume that POB to the power of γ and the internal field are direct proportion. Another issue is about the relation between the same lane and different lanes. Lateral movements of cars are not like vertical ones. No matter car or bus, lateral movements are lane-changing behaviors. It is better to define a threshold to control the movements about lane-changing behaviors. Because the problem about motorcycles in Taiwan is heavier and heavier, we retain the possibility to study the movements of motorcycles. For the purpose, we subdivide internal field into vertical and lateral field:

$$E_{\text{Internal}} = E_{\text{In},Lateral} + E_{\text{In},Vertical} \tag{3.2}$$

Figure 3-1 represents the lateral and vertical fields of vehicle 0 caused by vehicle 1 and vehicle 2:

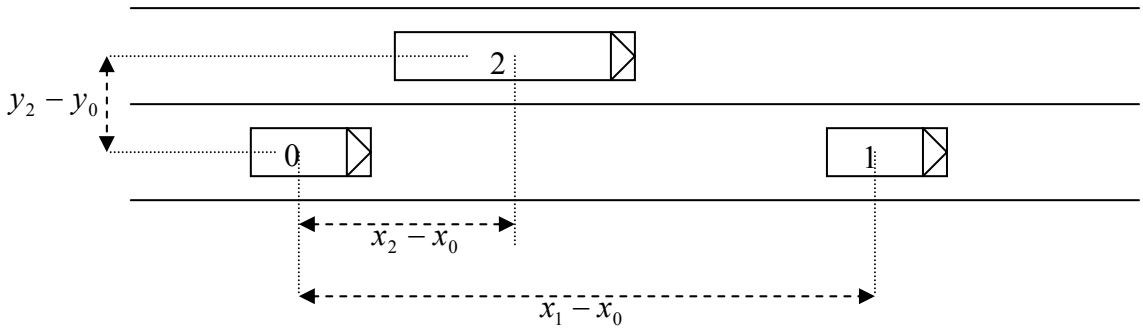

Figure 3-1 Internal fields between vehicles

For simplifying the model, we define the magnitude of vertical field to be M times of the lateral one. That is because drivers are more sensitive to vertical change in practical condition. A special phenomenon is that vertical fields must produce lateral force in traffic. It means that drivers will change lane if the leading cars move slowly or the distance between them is smaller than their safe distance. We assume the internal fields of vehicle 0 in Fig. 3-1 to be:

$$E_{0,IN,Vertical} = \frac{e_{10}}{\varepsilon}\left(\frac{u_{x,0}-u_{x,1}}{x_1-x_0}\right)^{\gamma} \tag{3.3a}$$

$$E_{0,In,Lateral} = \frac{1}{\varepsilon}\left[e_{10}\left(\frac{u_{x,0}-u_{x,1}}{x_1-x_0}\right)^{\gamma} - e_{20}\left(\frac{u_{x,0}-u_{x,2}}{x_2-x_0}\right)^{\gamma} - \frac{e_{20}}{M}\left(\frac{u_{y,0}-u_{y,2}}{y_2-y_0}\right)^{\gamma}\right] \tag{3.3b}$$

In Eq. (3.3a) and (3.3b), ε denotes the effect parameter, e_{10} and e_{20} denote the equivalents of vehicle 1 and vehicle 2 relative to vehicle 0. It must be especially noticed, the particle not only be affected by adjacent particles but all particles in the space in Newton's laws. However, cars are only affected by adjacent cars.

At the beginning of this section, we discuss two special cases to describe why we can't use Newton's laws in traffic. In Eq. (3.3a) and Eq. (3.3b), we neglect these two problems between adjacent cars. So we overcome the problems by defining *e* to be the function of speed difference between cars in this research. We also define a new variable δ. If the speed of the leading car is δ meter/second higher than the following car, still the following car accelerates even though they move closely. δ denotes a function of distance between adjacent cars. The relation between δ and the distance is inverse proportion. Because of above-mentioned assumptions, Eq. (3.3a) can be subdivided into Eq (3.3c) and Eq (3.3d)：

$$E_{0,In,Vertical} = \frac{[u_0-u_1+\delta(x_1-x_0)]}{\varepsilon}\left(\frac{u_0-u_1}{x_1-x_0}\right)^{\gamma} \quad \text{if } u_0-u_1+\delta(x_1-x_0)\geq 0 \tag{3.3c}$$

$$E_{0,In,Vertical} = 0 \quad \text{if } u_0-u_1+\delta(x_1-x_0)<0 \tag{3.3d}$$

The factors to affect δ will be discussed in following sections.

3.1.2 External Field

In section 3.1, we define the external field to be affected by external environments. Another evidence to prove the existence of external fields is that vehicle must accelerate or decelerate even though there is no car near it. It is convenient to define external field to be a function of desire speed. Unless driver reaches his desire speed, he would continue to change his velocity. The external field shows as follows:

$$E_{Ex,Vertical} = \frac{u_d - u_0}{t_d} \qquad (3.4)$$

In Eq. (3.4), $u_d = u_d(k, p_1, p_2.....)$, p denotes an environmental parameter, which includes gradient, weather, and so on. t_d denotes the time which the cars need to change it's velocity from u_0 to u_d.

3.1.3 Mobility

In this research, the meaning of mobility is the potential of drivers to change their status. It means the potential to accelerate, decelerate, and change lane. In following sections, mobility is a key parameter in traffic flow models. It decides each driver's choice about lane-changing behaviors and the magnitude of desired speed. The details of mobility will be discussed in following sections.

Before next section, it must be noticed that we don't care about lateral field. So the fields in following sections represent vertical (the way car moving) fields.

3.2 Behaviors and Simulator of Microscopic Models

One-dimension traffic flow models are most popular models, LWR and PW models are the most well-know two. In one-dimension models, cars are moving in alignment. It distributes all density in one line and simplifies traffic problems. We will calibrate the parameters in latest section and discuss the problems about muti-lane in next chapter.

We design a microscopic simulator to calibrate all parameters and verify the model which we have designed in last section. The assumptions in simulator are showed as follows:

(1) Transfer the density to be the amount of cars and put them in the road according to normal distribution.

(2) Distance between each car must be larger than a smallest distance (8 meters).

(3) The arrival of cars is based on Poisson distribution.

(4) The time step of the simulator is 3 seconds.

(5) The behaviors of cars refer to CA models.

We don't refer to Greenshields' or Greenberg's models in our simulator, so we need to define a series of reasonable moving behaviors:

(1) Each car has a maximum speed (free flow speed).

(2) Distance between each car must be larger than 8 meters.

(3) The speed of the following car shows as follows:

$$u_{follow}(t+\Delta t) = \min[u_f, u_{follow}(t) + rand \times \Delta t, \frac{x_{lead}(t) - x_{follow}(t)}{\Delta t} + \lambda \times \frac{(u_{lead}(t) + u_{lead}(t+\Delta t)}{2}] \quad (3.5)$$

(4) *rand* in Eq. (3.5) is calculated by Monte Carlo computing technique.

rand denotes a magnitude of acceleration. We calculate it by Monte Carlo computing technique to find the measurement of area in speed-time diagram.

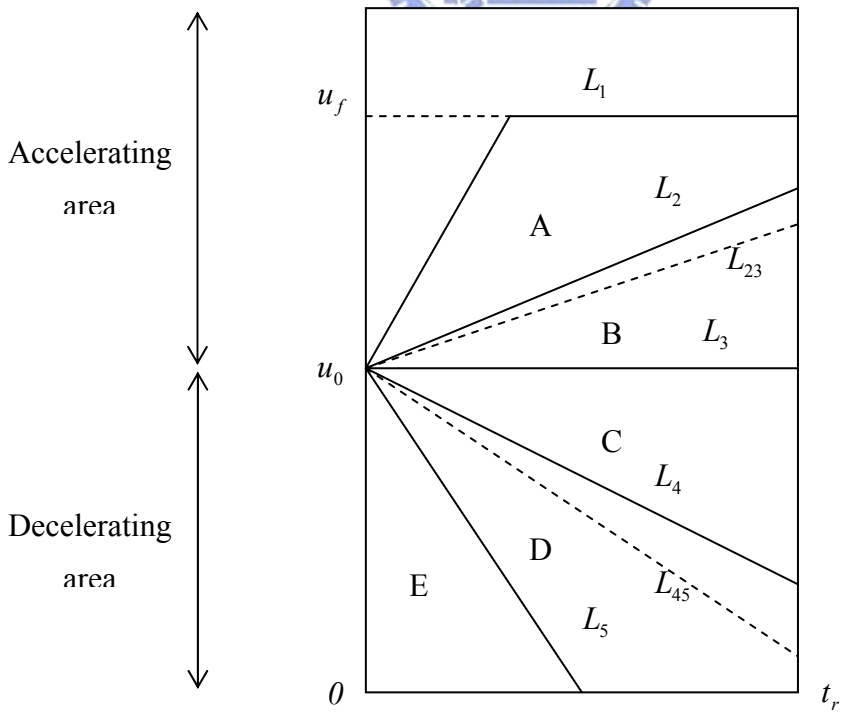

Figure 3-2

Speed-time diagram about Monte Carlo computing technique

We use Fig. 3-2 to define the magnitude of *rand*. In Fig. 3-2, the vertical axis denotes speed and the lateral axis denotes time, the measurement of area in Fig. 3-2 denotes distance. A, B, C, D, E represent areas, L_{23}, L_{45}, and $L_1 \sim L_5$ represent lines. u_f denotes free flow speed, u_0 denotes the speed of the following car at time 0, and t_r denotes the time step of simulator. The meanings of each lines are showed as table 3-1:

Table 3-1 The meanings of each line in Fig.3-2

L_1	Maximum accelerating line of the following car
L_2	The upper-bound keeps the following car to avoid bumping into the leading car
L_3	The line represents that the following car maintains a constant speed
L_4	The lower-bound keeps the following car to avoid bumping into the leading car
L_5	Maximum decelerating line of the following car

Fig. 3-2 is an example for explaining the meanings of each line. All procedures are described as follows:

1. The bound condition which avoids accident is showed as Eq. (3.6):

$$u_{follow}(t)\cdot\Delta t \le x_{lead}(t) - x_{lag}(t) + \lambda \times \frac{\Delta t\cdot(u_{lead}(t)+u_{lead}(t+\Delta t)}{2} \qquad (3.6)$$

If Eq. (3.6) is satisfied, we simulate the accelerate area because no accident happens. On the other hand, if any accident happens, we simulate the decelerate area.

2. We set a variable k=0 and put *N* points in accelerating area (or decelerate area according to step 1) randomly. After that, we connect every point to origin (where time and speed equal to 0). Once a connecting line limits to maximum accelerating line to avoid bumping into leading car, set k=k+1. (In Fig. 3-2, B represents the accelerating area and C represents the decelerating area where the following cars would not bump into the leading car.) Finally, $k/N \times$ accelerating area (or decelerating area) is the satisfied area.

3. The satisfied area calculated in step 2 and original area (C, D, and E if in accelerating area, E if in decelerating area) are combined to be a total area. We draw an approximate line (L_{23} and L_{45} in Fig. 3-2) and get an area around approximate line and L_3. If the area is the same as total area, the approximate line will be the acceleration at that time step.

The maximum difference between Eq. (3.6) and CA models is the latest term in Eq. (3.6). We introduce λ (mobility) into latest term to represent drivers' perception of the leading cars. The range of mobility is from 0 to 1. Besides, for describing drivers' behaviors well, time step of simulator is designed to be 3 seconds. That is because cars need enough time to react to the leading cars such as to decelerate or change lane. But 3 seconds is too long for the version of CA. If we don't introduce mobility into the latest term of Eq. (3.6), cars will move 3 seconds and stop 3 seconds when traffic is heavy. The magnitude of mobility is defined randomly in the simulator. The flowchart of simulator is showed as Fig. 3-3:

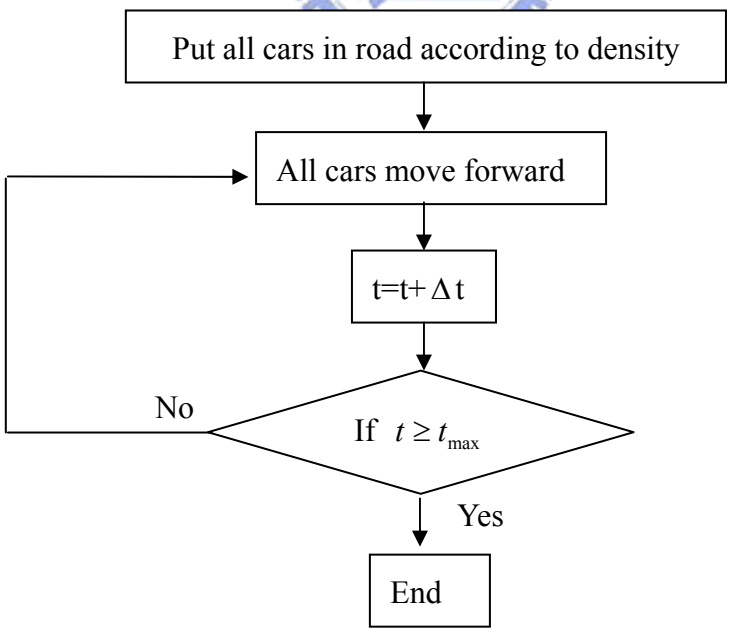

Figure 3-3 The flowchart of 1-D simulator

3.3 Calibration of the Parameters and Verification of the Model

In this section, we calibrate all parameters in the models based on the simulator designed in last section. Main equations are (3.3c) and (3.3d) and main parameters are ε and δ.

3.3.1 Calibration of δ

δ is a magnitude of speed. When the speed of the leading car is δ meter/ second larger than the following one, the following car will accelerate even though two adjacent cars are near. It is obvious that δ and the distance between two cars must be inverse proportion. It means that when two cars are nearer, speed of the leading car must be higher to make the following one to accelerate. Of course, δ is not only affected by the distance between two cars. We can find out the other factors rely on simulator.

For simplifying the data, we sift useless data from the output of the simulator. The data we need must satisfy the following constraints:

1. Accelerating behaviors
2. Total magnitude of acceleration must be larger than the magnitude only caused by external field.

After that, we get Fig. 3-4:

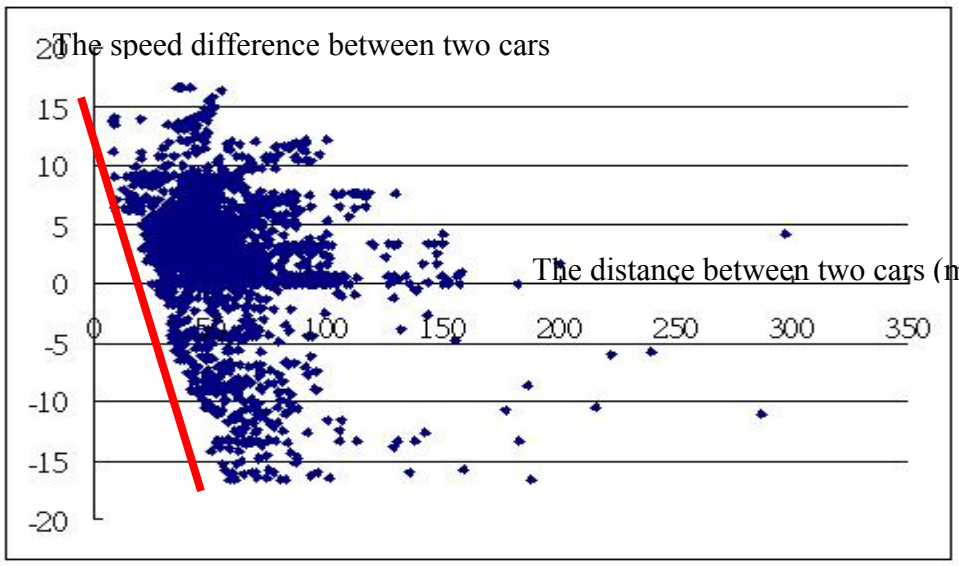

Figure 3-4

The relation between the distance and speed difference of two adjacent cars

In Fig. 3-4, the lateral axis denotes the distance between two adjacent cars and the vertical axis denotes the speed difference between them. The free flow speed is 60 Km / hour and the jam density is 125 vehicle /Km. The range of mobility is from 0.1 to 0.4. We can find that the gradient of straight line in Fig. 3-4 is δ and which is calculated in Eq. (3.7):

$$\delta = u_f - \frac{2\cdot(x_1 - x_0)}{\Delta t \cdot u_f} u_f = u_f - \frac{2\cdot(x_1 - x_0)}{\Delta t} \tag{3.7}$$

For finding out the relation between δ and mobility, we subdivide Fig. 3-4 into Fig. 3-5:

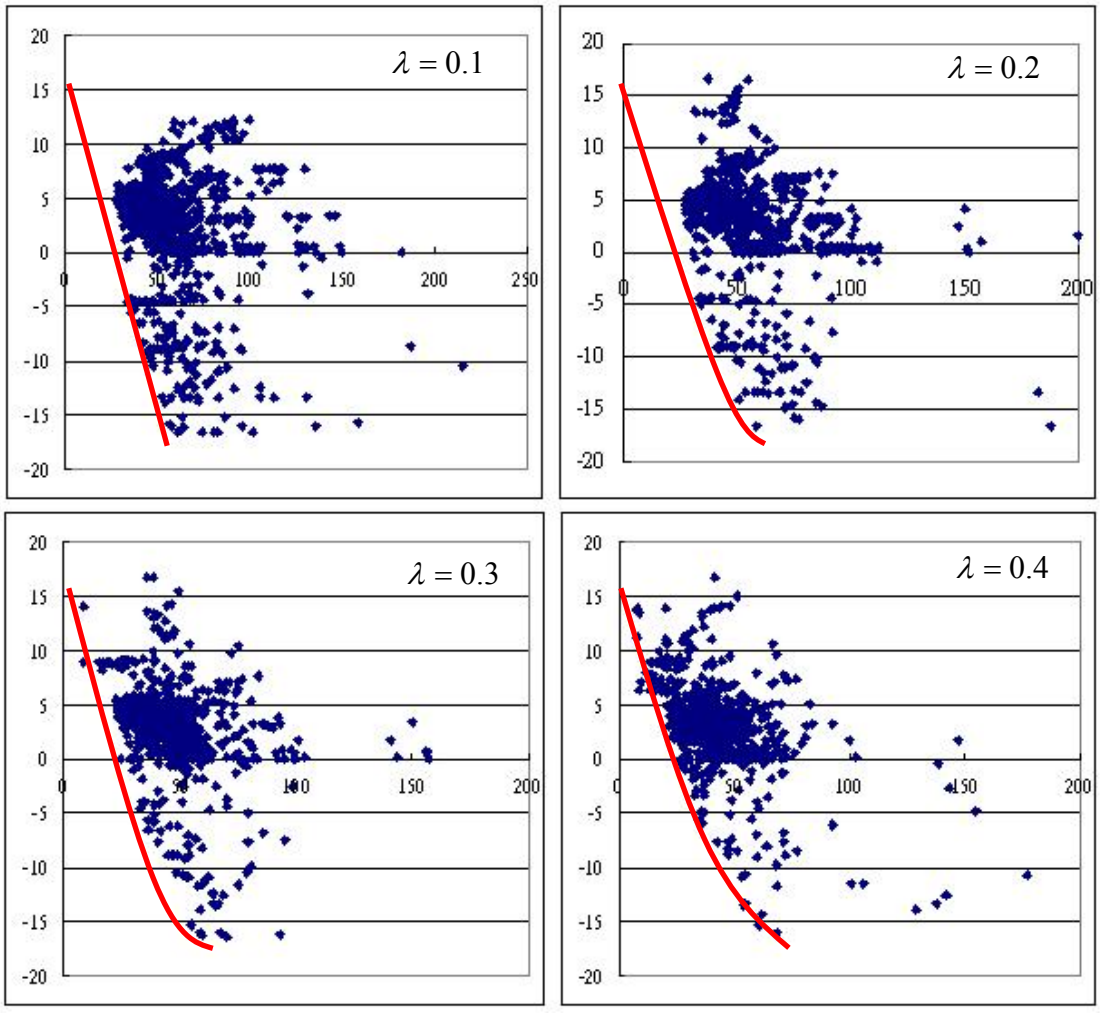

Figure 3-5

The relation between δ and mobility

Because we only retain the data with no internal field, Fig. 3-5 is an expected result. We know that the behaviors of drivers are affected by mobility if the internal fields exit (see Eq. 3.5). The phenomenon is proved again by the result of simulator.

3.3.2 Calibration of γ

γ denotes a parameter which represents the relation between the POB and the internal fields. We rewrite Eq. (3.3) to get Eq. (3.8)

$$\frac{E_{0,\mathrm{In}}}{[u_0 - u_1 + \delta(x_1 - x_0)]} = \frac{1}{\varepsilon}\left(\frac{u_0 - u_1}{x_1 - x_0}\right)^{\gamma} \qquad \text{if } u_0 - u_1 + \delta(x_1 - x_0) \geq 0 \qquad (3.8)$$

We change the vertical and lateral axis to obtain Fig. 3-6:

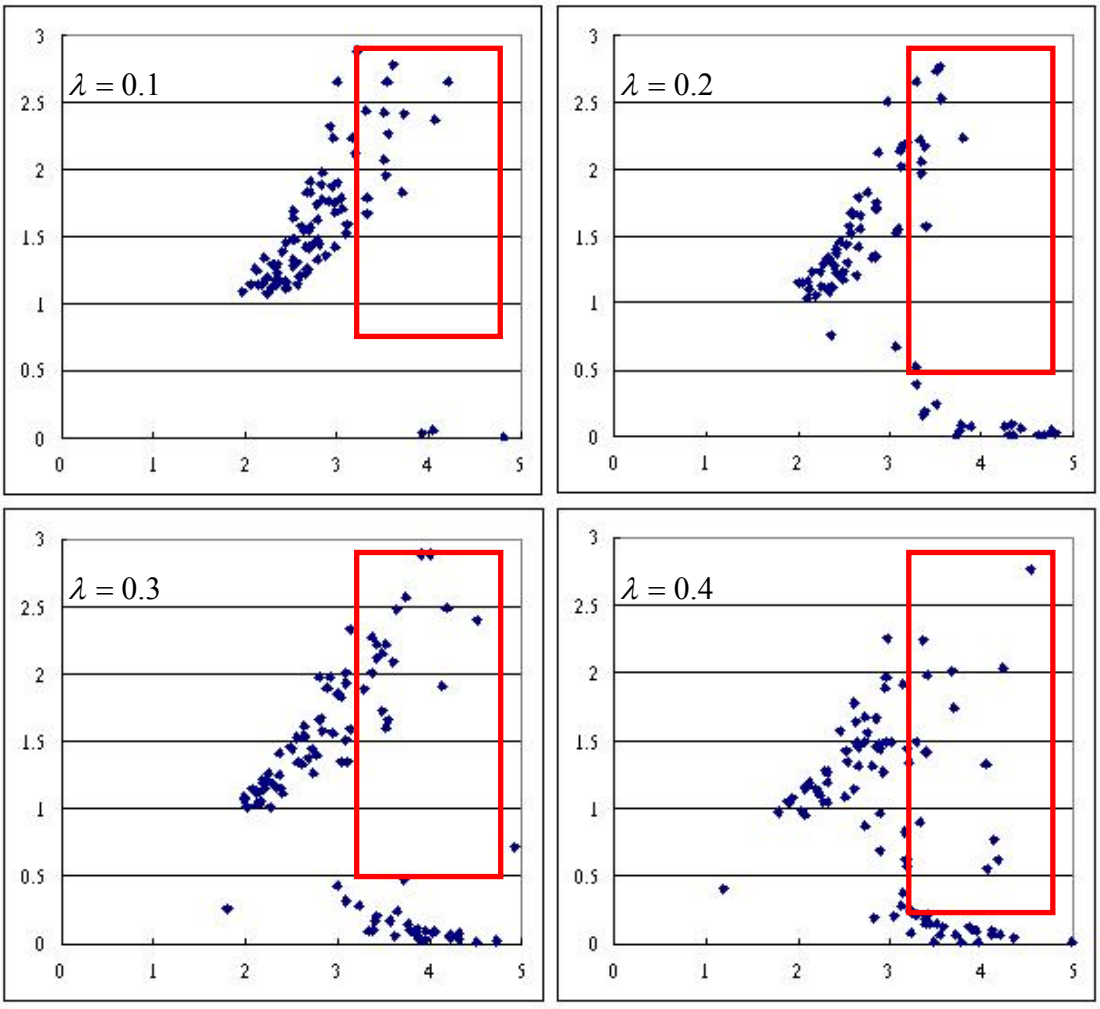

Figure 3-6

Unreasonable relation between POB and the internal fields

In Fig 3-6, the vertical axis denotes the POB which is calculated from $x_1 - x_0 \big/ u_0 - u_1$. The unit of it is second. The Lateral axis is calculated from $E_{0,\mathrm{In}} \big/ (u_0 - u_1 + \delta(x_1 - x_2))$.

The result of Fig. 3-6 is unreasonable because the points in the frame should not exit. It means that to calculate POB from $x_1 - x_0 \big/ u_0 - u_1$ is unsuitable. There is high speed in these points to lead to smaller $u_0 - u_1$. The phenomenon also leads to a larger POB indirectly but it should not exit in practical condition.

The unreasonable phenomenon exits because we neglect the effects of mobility when we calculate the POB. In practical condition, the following driver has an ability to predict the trace of the leading car. Once the driver of the following car can predict the trace of the leading car, the POB will be smaller. Mobility also affects the ability to predict. Radical drivers (with high mobility) have smaller POB but conservative drivers (low mobility) have higher POB. According to the assumptions, we must redefine the formulation of POB showed as Eq. (3.9)

$$Probability\ \ of\ \ bump = \frac{x_1 - x_0}{u_0 - \lambda \cdot u_1} \qquad (3.9)$$

According to Eq. (3.9), we obtain Fig. 3-7 from Fig. 3-6:

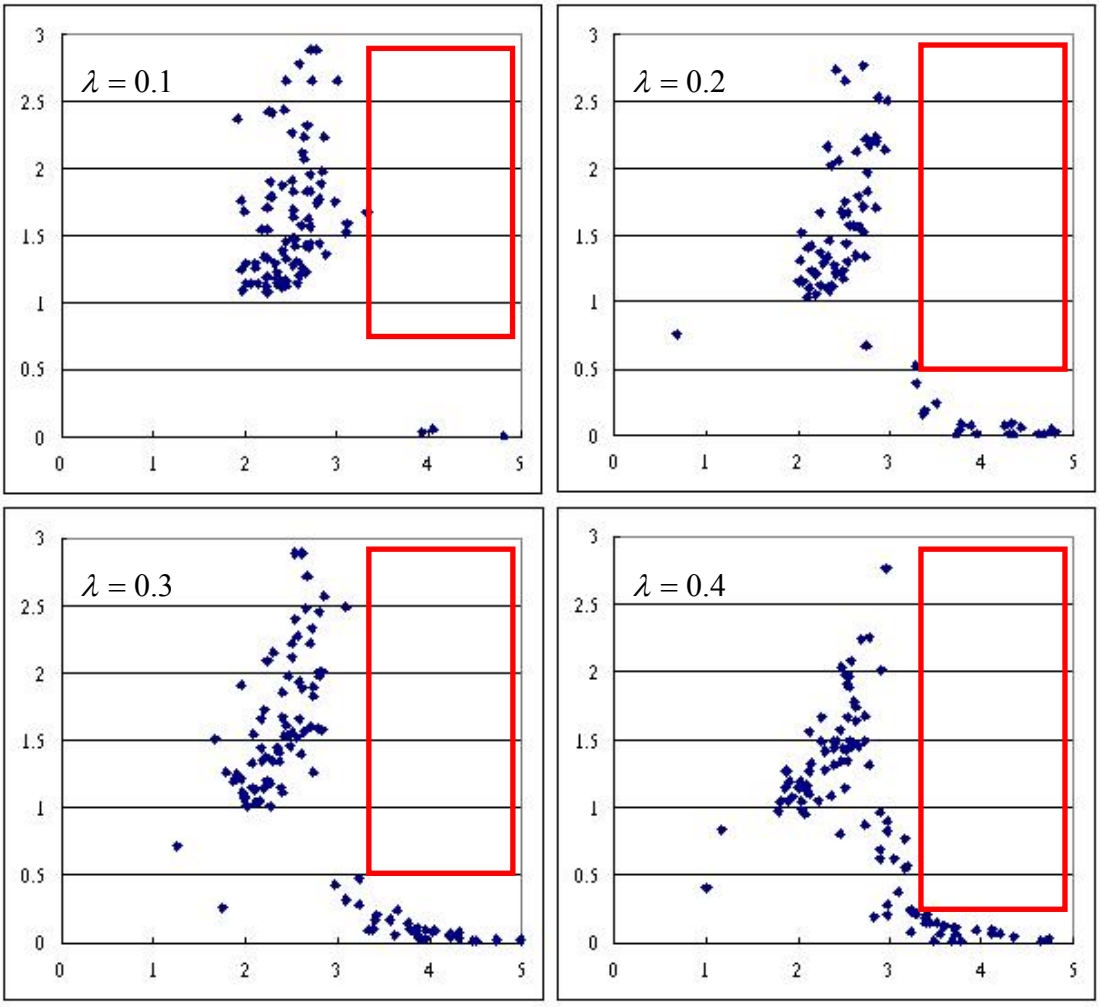

Figure 3-7

Reasonable relation between the POB and the internal fields

There is an important message in Fig. 3-7. For the purpose to analyze the relation between the POB and the internal fields, we must discuss two conditions separately. These two conditions depend on whether the POB is larger than the time step. Because time step is 3 seconds in this research, Fig. 3-7 must be segmented into Fig. 3-8 and Fig. 3-9:

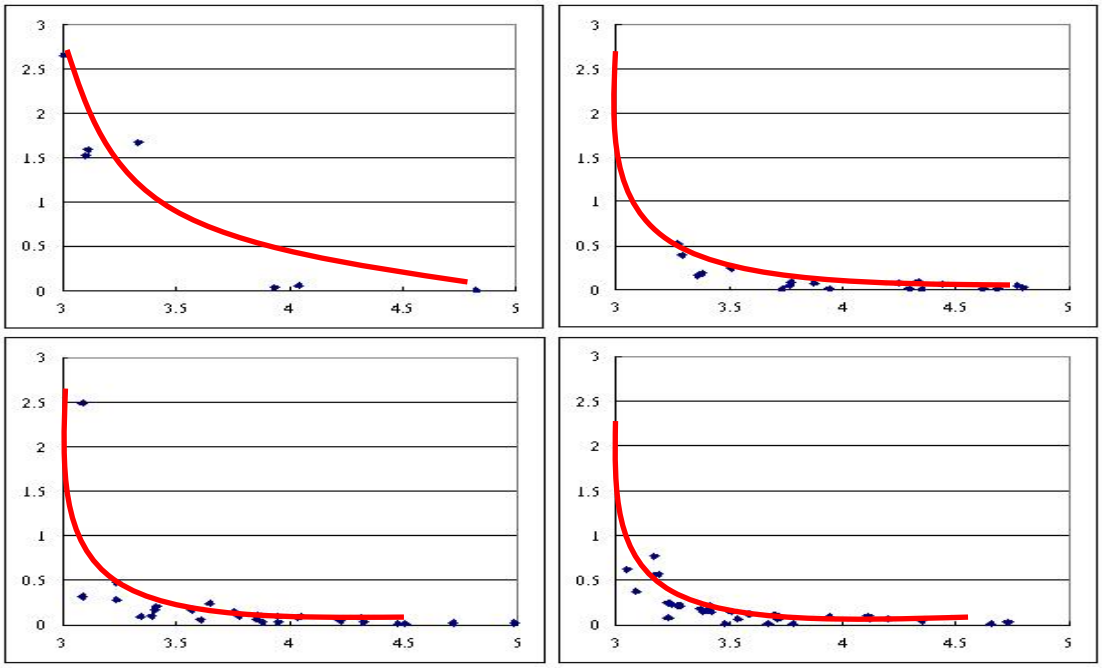

Figure 3-8

The relation between the POB and the internal fields

(When the POB is larger than the time step)

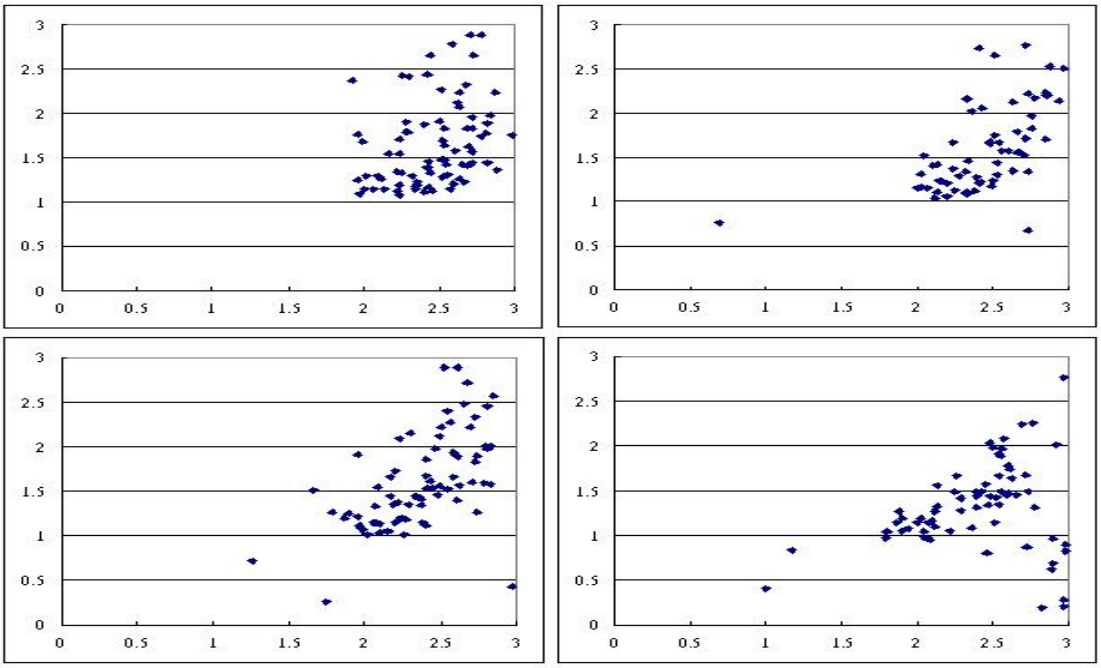

Figure 3-9

The relation between the POB and the internal fields

(When the POB is smaller than the time step)

In Fig. 3-8, when the POB is smaller, deceleration is larger and vice versa. In Fig. 3-9, it seems that the distribution of points is irregular. In fact, if the POB is smaller than the time step, drivers must decelerate to avoid bumping into the leading cars. When the time step is smaller, the phenomenon is more obvious. When mobility is larger, the phenomenon is more unobvious. So, we formulate the relation between the POB and the internal fields showed as Eq. (3.10a) and Eq. (3.10b):

$$\frac{E_{0,In}}{u_0 - u_1 + \delta(x_1 - x_0)} = \frac{1}{\varepsilon}\left(\frac{u_0 - \lambda \cdot u_1}{x_1 - x_0}\right)^{\gamma} \quad \text{if} \quad \frac{x_1 - x_0}{u_0 - \lambda \cdot u_1} \geq \Delta t \tag{3.10a}$$

$$E_{0,In} = -E_{0,Ex} - u_0 \quad \text{if} \quad \frac{x_1 - x_0}{u_0 - \lambda \cdot u_1} < \Delta t \tag{3.10b}$$

We also finds out that when mobility λ is larger, γ is larger from the result of simulator. According to the curves in Fig. 3-8, we define $\gamma = 1 + 10\lambda$ roughly to calibrate ε in next section.

3.3.3 Calibration of ε

Before calibrating ε, we review Eq. (3.3), (3.7), and (3.10) to formulate microscopic internal fields showed as Eq. (3.11):

$$E_{0,\mathrm{In}} = \frac{[u_0 - u_1 + \delta(x_1 - x_0)]}{\varepsilon}\left(\frac{u_0 - \lambda \cdot u_1}{x_1 - x_0}\right)^{\gamma}$$

$$\text{if } u_0 - u_1 + \delta(x_1 - x_0) \geq 0 \text{ and } \frac{x_1 - x_0}{u_0 - \lambda \cdot u_1} \geq \Delta t \tag{3.11a}$$

$$E_{0,In} = -E_{0,Ex} - u_0$$

$$\text{if } u_0 - u_1 + \delta(x_1 - x_0) \geq 0 \text{ and } \frac{x_1 - x_0}{u_0 - \lambda \cdot u_1} < \Delta t \tag{3.11b}$$

$$E_{0,\mathrm{In}} = 0 \quad \text{if } u_0 - u_1 + \delta(x_1 - x_0) < 0 \tag{3.11c}$$

$$\delta(x_1 - x_0) = u_f - \frac{2 \cdot (x_1 - x_0)}{\Delta t} \tag{3.11d}$$

$$\gamma = 1 + 10\lambda \tag{3.11e}$$

According to Eq. (3.11) and the result of simulator, the calibration of $1/\varepsilon$ is showed as Fig. 3-10

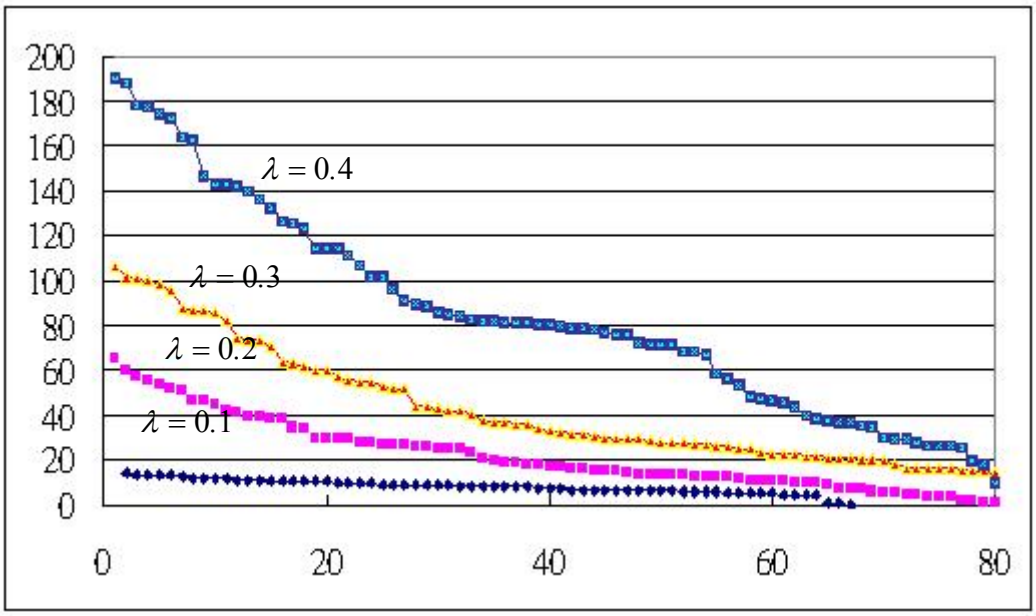

Figure 3-10 The magnitude of $1/\varepsilon$ with different mobility

In Fig. 3-10, the vertical axis denotes different samples and the lateral axis denotes the magnitude of $1/\varepsilon$. It is obviously that $1/\varepsilon$ is affected by mobility. For simplifying models, we define different magnitude of $1/\varepsilon$ according to different mobility. The result of simulator is showed in Table 3-2:

Table3-2 Statistic date of $1/\varepsilon$ and mobility

Magnitude of mobility	Average of $1/\varepsilon$	Standard deviation of $1/\varepsilon$
0.1	10.20	3.84
0.2	22.14	15.84
0.3	35.58	20.25
0.4	75.52	43.20

3.4 Macroscopic Single-Lane Models

Eq. (3.4) and (3.11) represent microscopic models. For calculating real-time informations, macroscopic models are needed especially to simulate large scale network.

3.4.1 Macroscopic Internal Fields

The distance between cars in microscopic models is a reciprocal of the density in macroscopic ones. The derivation of macroscopic internal fields is showed as follows:

$$
\begin{aligned}
E_{\text{In}} &= \frac{[u_0 - u_1 + \delta(x_1 - x_0)]}{\varepsilon}\left(\frac{u_0 - \lambda \cdot u_1}{x_1 - x_0}\right)^{\gamma} \\
&= \frac{[u_0 - u_1 + \delta(x_1 - x_0)]}{\varepsilon} \cdot \eta(\lambda) \cdot \left(\frac{u_0 - u_1}{x_1 - x_0}\right)^{\gamma} \\
&= \frac{\eta(\lambda)}{\varepsilon}\frac{(u_0 - u_1)^{\gamma+1}}{(x_1 - x_0)^{\gamma}} + \frac{\eta(\lambda)}{\varepsilon}\frac{\delta(x_1 - x_0)(u_0 - u_1)^{\gamma}}{(x_1 - x_0)^{\gamma}} \\
&= \frac{\eta(\lambda)}{\varepsilon}\frac{(u_0 - u_1)^{\gamma+1}}{(x_1 - x_0)^{\gamma}} + \frac{\eta(\lambda)}{\varepsilon}\delta(x_1 - x_0)\left(\frac{u_0 - u_1}{x_1 - x_0}\right)^{\gamma} \\
&= -\frac{\eta(\lambda)}{\varepsilon}\frac{(u_1 - u_0)^{\gamma+1}}{(x_1 - x_0)^{\gamma+1}}(x_1 - x_0) - \frac{\eta(\lambda)}{\varepsilon}\delta(x_1 - x_0)\left(\frac{u_1 - u_0}{x_1 - x_0}\right)^{\gamma} \\
&= -\frac{\eta(\lambda)}{\varepsilon}\frac{\partial u^{\gamma'}}{\partial x^{\gamma'}}k - \frac{\eta(\lambda)}{\varepsilon}\delta(k)\frac{\partial u^{\gamma}}{\partial x^{\gamma}}
\end{aligned}
$$

Conditional parts are showed as follows:

$$
\begin{aligned}
& u_0 - u_1 + \delta(x_1 - x_0) \geq 0 \\
\Rightarrow\ & \frac{u_0 - u_1}{x_1 - x_0} + \frac{\delta(x_1 - x_0)}{x_1 - x_0} \geq 0 \\
\Rightarrow\ & -\frac{\partial u}{\partial x} + \delta'(k) \geq 0
\end{aligned}
$$

$$\frac{x_1 - x_0}{u_0 - \lambda \cdot u_1} \geq \Delta t$$
$$\Rightarrow \frac{u_0 - \lambda \cdot u_1}{x_1 - x_0} \leq \frac{1}{\Delta t}$$
$$\Rightarrow \eta(\lambda)(\frac{u_0 - u_1}{x_1 - x_0}) \leq \frac{1}{\Delta t}$$
$$\Rightarrow -\eta(\lambda)\frac{\partial u}{\partial x} \leq \frac{1}{\Delta}$$

According to above-mentioned derivations, Eq. (3.12a) is obtained:

$$E_{\text{In}} = -\frac{\eta(\lambda)}{\varepsilon}\frac{\partial u^{\gamma'}}{\partial x^{\gamma'}}k - \frac{\eta(\lambda)}{\varepsilon}\delta(k)\frac{\partial u^{\gamma}}{\partial x^{\gamma}} \qquad \text{if } -\frac{\partial u}{\partial x} + \delta'(k) \geq 0 \text{ and } -\eta(\lambda)\frac{\partial u}{\partial x} \leq \frac{1}{\Delta} \tag{3.12a}$$

In Eq. (3.12a), $\gamma' = \gamma + 1$, $\delta'(k)$, $\eta(\lambda)$, and Δ are additional variables and parameters.

According to Eq. (3.7):

$$\delta'(k) = \frac{u_f}{x_1 - x_0} - \frac{2}{\Delta} = u_f \cdot k - 2/\Delta \tag{3-12b}$$

Δ denotes the time step. According to above-mentioned derivations, we obtain:

$$\eta(\lambda)\frac{u_0 - u_1}{x_1 - x_0} = \frac{u_0 - \lambda \cdot u_1}{x_1 - x_0}$$
$$\Rightarrow \eta(\lambda) = \frac{u_0 - \lambda \cdot u_1}{u_0 - u_1} \geq \frac{u_0 - u_1}{u_0 - u_1} = 1$$

Because the range of λ is from 0 to 1, $\eta(\lambda)$ must be larger than 1. The result of simulator is showed in Table 3-3:

Table3-3 Statistic data of $\eta(\lambda)$ and mobility

Mobility	Average of $\eta(\lambda)$	Standard deviation of $\eta(\lambda)$
0.1	1.295	0.254
0.2	1.242	0.383
0.3	1.386	0.512
0.4	1.360	0.659

Table 3-3 represents that the standard deviation of $\eta(\lambda)$ only be affected by mobility. If the internal fields are Eq. (3.11b) and (3.11c), we obtain:

$$E_{In} = -E_{Ex} - u \qquad if\text{-}\frac{\partial u}{\partial x} + \delta'(k) \geq 0 \text{ and} - \eta(\lambda)\frac{\partial u}{\partial x} \leq \frac{1}{\Delta} \qquad (3.12b)$$

$$E_{\text{In}} = 0 \qquad if\ \frac{\partial u}{\partial x} + \delta'(k) < 0 \qquad (3.12c)$$

In Eq. (3.12a) and (3.12b), δ' and δ can also be represented by $\delta'(1/k)$ and $\delta(1/k)$.

3.4.2 Macroscopic External Field

We define the microscopic external field to be a function of each driver's desire speed. But it needs aggregate variables to represent macroscopic models. We introduce the well-know relaxation-term to describe the external field in this research. It must be noticed that the equilibrium velocity would not only be the function of density. Some external environments must be taken into account, too. Formulation of the external field is showed as Eq. (3.13):

$$E_{Ex,Vertical} = \frac{u_e - u}{T} \qquad (3.13)$$

In Eq. (3.13), $u_e = u_e(k, p_1, p_2.....)$, p denotes the external environments such as gradient, weather, and so on. Because there is no data to calibrate equilibrium velocity, we introduce May's definition (1967):

$$u_e = u_f\ exp(\frac{k}{k_j})^{-0.5} \qquad (3.14)$$

3.4.3 Summary

All procedures about simulation are showed as follows:

（1） Define the type of the internal field according to the different thresholds.

（2） Choice a magnitude of $\eta(\lambda)$ according to Table 3-5

（3） Choice a magnitude of $1/\varepsilon$ according to Table 3-4

（4） Define the behaviors of cars according to the external fields and some other

parameters.

The macroscopic model is showed as Eq. (3.15):

$$\frac{\partial q}{\partial x}+\frac{\partial k}{\partial t}=0 \text{ 、 } \frac{du}{dt}=E_{In}+E_{Ex} \text{ 、 } q=ku$$

$$E_{\mathrm{In}}=-\frac{\eta(\lambda)}{\varepsilon}\frac{\partial u^{\gamma'}}{\partial x^{\gamma'}}k-\frac{\eta(\lambda)}{\varepsilon}\delta(k)\frac{\partial u^{\gamma}}{\partial x^{\gamma}} \qquad \text{if } -\frac{\partial u}{\partial x}+\delta'(k)\geq 0 \text{ and } -\eta(\lambda)\frac{\partial u}{\partial x}\leq\frac{1}{\Delta}$$

$$E_{In}=-E_{Ex}-u \qquad \text{if } -\frac{\partial u}{\partial x}+\delta'(k)\geq 0 \text{ and } -\eta(\lambda)\frac{\partial u}{\partial x}\leq\frac{1}{\Delta}$$

$$E_{\mathrm{In}}=0 \qquad if\ \frac{\partial u}{\partial x}+\delta'(k)<0$$

$$E_{Ex}=\frac{u_e-u}{T} \text{ 、 } \delta'(k)=u_f\cdot k-2/\Delta \text{ 、 } u_e=u_f\,exp(\frac{k}{k_j})^{-0.5} \text{ 、 } \gamma'=1+\gamma=2+10\lambda \qquad (3.15)$$

CHAPTER 4
Multi-Lane Traffic Flow Model

We derive a multi-lane traffic flow model in Chapter 4, which is combined with several 1-demension single lane traffic flow models. These kinds of models had been published by Michalopoulos, etc. (1980), maximum difference of these kinds of models is that the right-hand-side term of the conservation equation is not zero. Lane-changing flow rate must be defined in these kinds of models. But we think not only conservation equation should be corrected but also motion equation, too.

The key point is that the shock caused by different lanes is larger than the shock caused by original lane when the amount of changing density is the same:

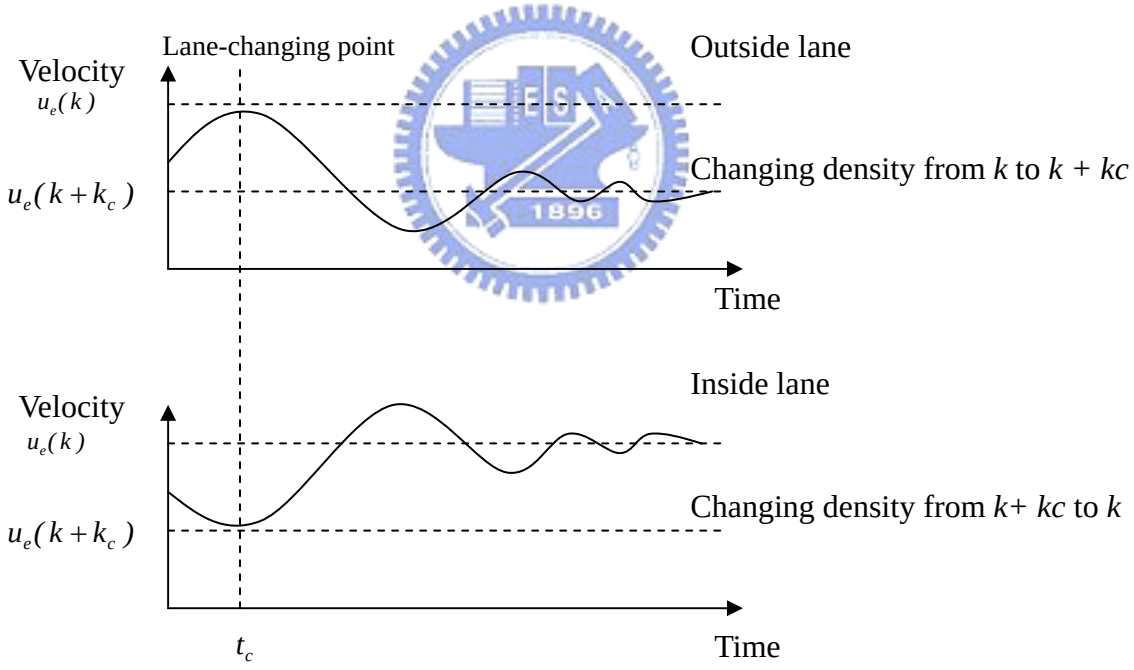

Figure 4-1 The shock caused by lane-changing behaviors

Fig. 4-1 represents the change of density when the lane-changing behaviors happen. In Fig. 4-1, the vertical axis denotes the time, and the lateral one denotes velocity. If the initial velocity of inside and outside lane are the same and the density are $k + k_c$ and k. t_c is the time that the lane-changing behaviors happen. Before t_c, the velocity of

inside and outside lane change toward its' equilibrium velocity. After t_c, the amount of density(*kc*) shifts from inside lane to outside lane and causes large shock to traffic. So, we adjust not only conservation equation but also motion equation to satisfy above-mentioned phenomenon. We will describe the details of multi-lane simulator in the first section of this chapter. We design a microscopic multi-lane traffic flow model and discuss the shock caused by lane-changing behaviors in the second section. We transfer the microscopic model to be the macroscopic one and verify its' parameter in latest section.

4.1 Microscopic Behaviors and Simulator

In this section, we describe the behaviors of drivers in multi-lane models and define the lane-changing constraints. The relation between mobility and the lane-changing behaviors will be discussed, too. Besides, an additional variable "driver's inertia" will be explained in 4.1.2.

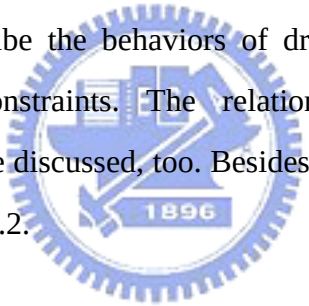

4.1.1 The Lane-Changing Constraints

There is a series of constraints for drivers to judge whether they change lane in the multi-lane models. In this research, we define three constraints:

1. When drivers do lane-changing behaviors, it must increase the distance between them and the leading car.
2. If a driver wants to change lane, he must consider the distance between him and the car behind him in target lane.
3. There must be an interval of designed time between each lane-changing behaviors of the same car. It means that drivers can not change lane at every time step,

The purpose of third constraint is to avoid ping-pong phenomenon. Of course, all constraints will be affected by mobility in this research.

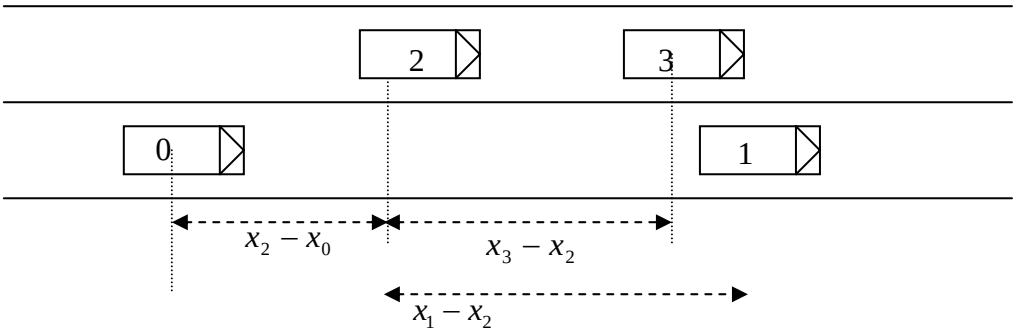

Figure 4-2

An example about the lane-changing constraints

In Fig.4-2, vehicle 2 is our target. If vehicle 2 wants to change lane, it must satisfy the following constraints:

$$x_1 - x_2 \geq (x_3 - x_2) \cdot [1 + (\lambda_{max} - \lambda_2)] \tag{4.1}$$

$$x_2 - x_0 \geq \frac{[u_0 + (\lambda_{max} - \lambda_2) \cdot u_0] \cdot \Delta t}{2} \tag{4.2}$$

$$t_{2,nochange} \geq (\lambda_{\max} - \lambda_2) \cdot t_{nochange} \tag{4.3}$$

In Eq. (4.1), (4.2). and (4.3), $\lambda_{\max}$ is 1 in our simulator (the range of mobility is from 0 to 1). It is obviously that drivers with high mobility have low thresholds to limit them doing lane-changing behaviors.

4.1.2 Driver's Inertia

When the following cars move with constant leading cars for a long time, drivers of the following cars can predict the behaviors of the leading cars more exactly. Driver's inertia represents above-mentioned phenomenon. The magnitude of driver's inertia will increase when the following time increases. In the single lane models, driver's inertia is 1. But the lane-changing behaviors appear in multi-lane models. Once a driver change lane, he can not predict the behaviors of the car in front of him well immediately. So, we adjust Eq. (3.5) to be Eq. (4.4):

$$u_{follow}(t+\Delta t) = \min[u_f, u_{follow}(t) + rand \times \Delta t, \frac{x_{lead}(t) - x_{follow}(t)}{\Delta t} + \phi \times \lambda \times \frac{u_{lead}(t) + u_{lead}(t+\Delta t)}{2}] \quad (4.4)$$

ϕ denotes the driver's inertia. We define that every drivers need three time steps to predict the behaviors of the leading cars completely. So, Eq. (4.5) is obtained:

$$\phi = Min[1, t'/3] \quad (4.5)$$

t' is the number of time step.

4.1.3 The Procedures of Simulator

According to 4.1.1 and 4.1.2, the assumptions of microscopic multi-lane models are:

(1) Transfer the density to be the amount of cars and put them in the road according to normal distribution.

(2) The distance between each car must be larger than a smallest distance (8 meters).

(3) The arrival of cars is defined based on Poisson distribution.

(4) The time step of simulator is 3 seconds.

(5) The behaviors of cars refer to CA models.

(6) In a time step, cars move forward first and then change lane.

We don't refer to Greenshields' or Greenberg's models in our simulator, so we define a series of reasonable moving behaviors:

(1) Each car has a maximum speed (free flow speed).

(2) The distance between each car must be larger than 8 meters.

(3) Eq. (4.4) represents the speed of following car.

(4) *rand* in Eq. (4.4) is calculated by Monte Carlo computing technique which has been described in chapter 3.

(5) Eq. (4.1), (4.2), and (4.3) must be satisfied if cars want to change lane.

The flowchart of simulator is showed as follows:

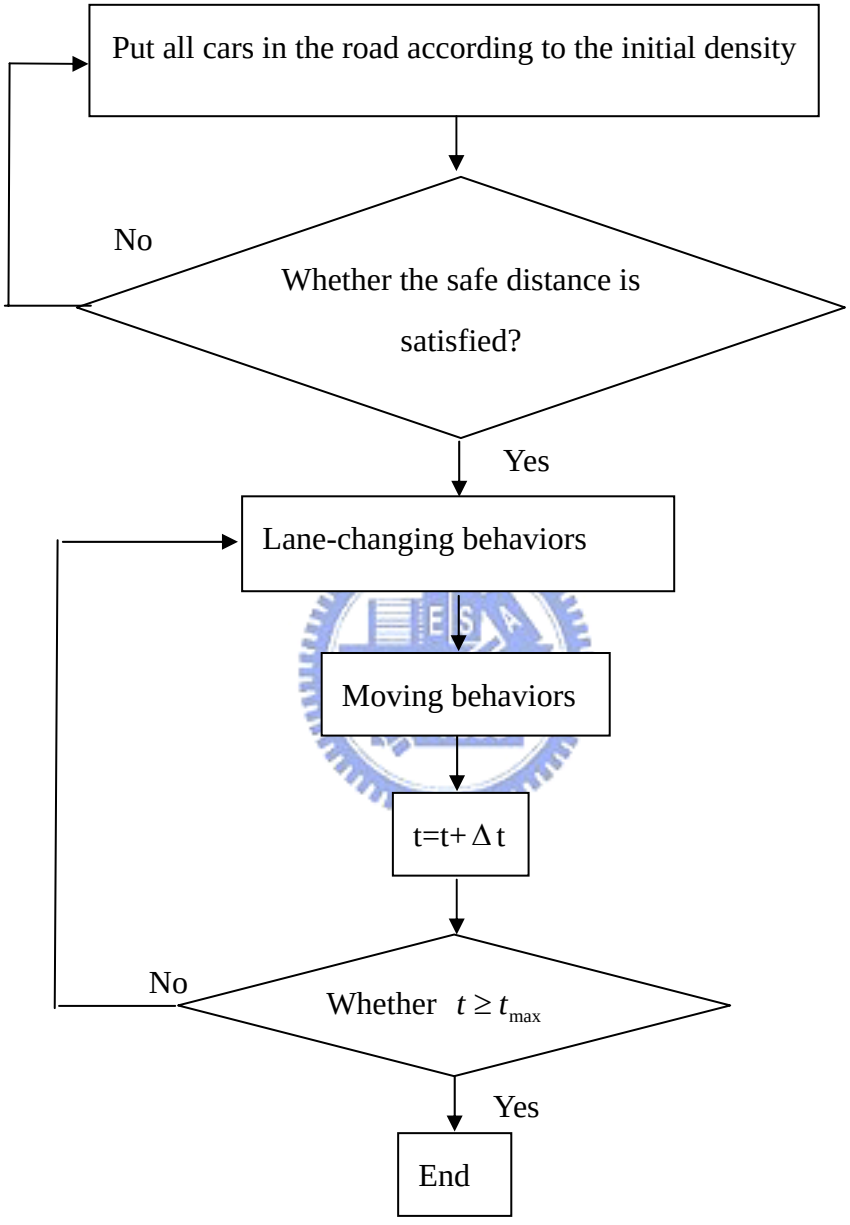

Figure 4-3

The flowchart of multi-lane simulator

The details of lane-changing behaviors are showed in Fig. (4-4):

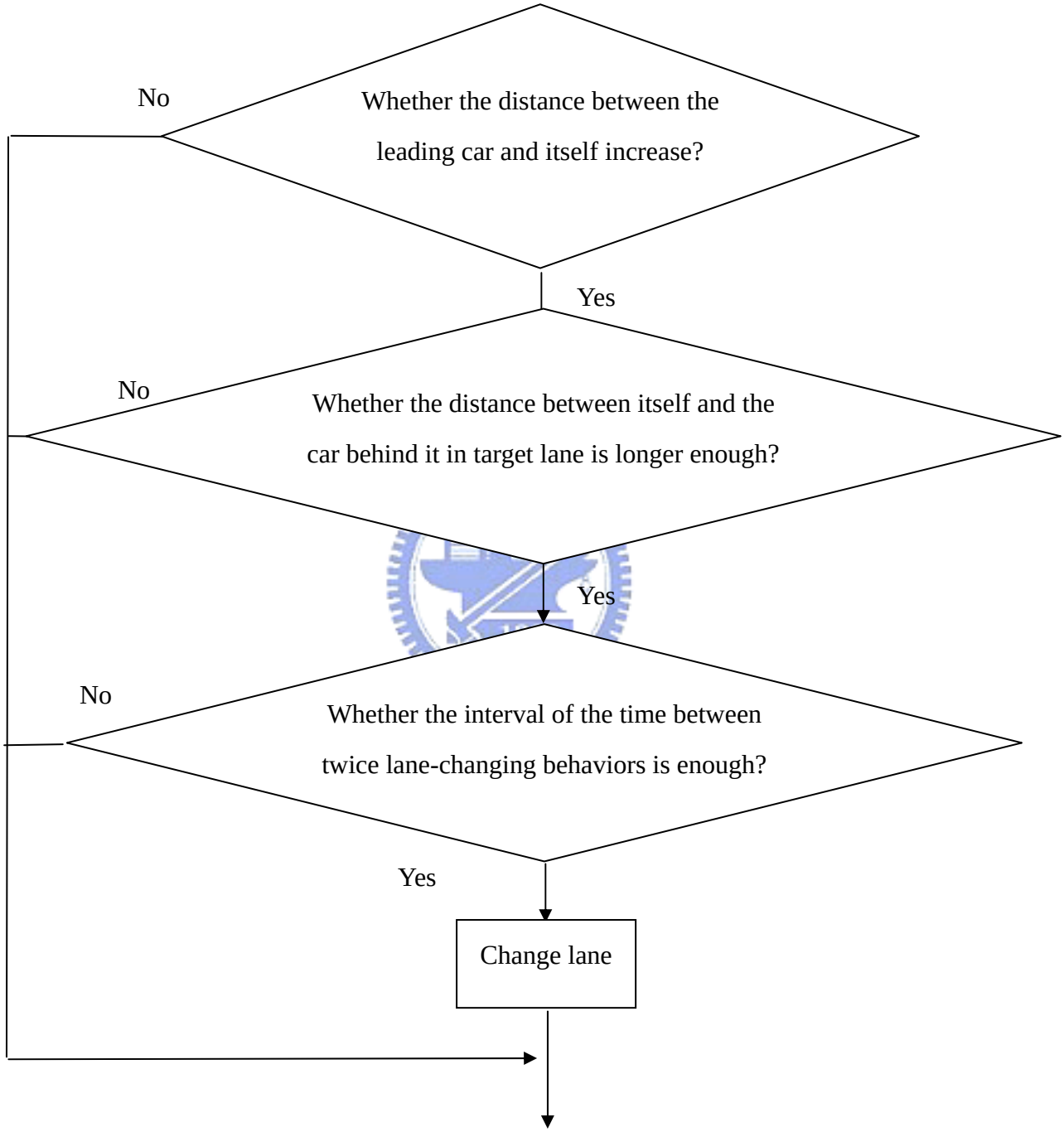

Figure 4-4

Flowchart of the lane-changing judgment

4.2 Microscopic Multi-Lane Traffic Flow Model

There are different internal fields from single lane models in multi-lane models . We review the internal fields of the single lane models:

$$E_{0,\mathrm{In}} = \frac{[u_0 - u_1 + \delta(x_1 - x_0)]}{\varepsilon}\left(\frac{u_0 - \lambda \cdot u_1}{x_1 - x_0}\right)^{\gamma}$$

$$\text{if } \; u_0 - u_1 + \delta(x_1 - x_0) \geq 0 \;\; \text{and} \;\; \frac{x_1 - x_0}{u_0 - \lambda \cdot u_1} \geq \Delta t \qquad (3.11a)$$

First, we introduce driver's inertia into Eq. (3.11a):

$$E_{0,\mathrm{In}} = \frac{[u_0 - u_1 + \delta(x_1 - x_0)]}{\varepsilon}\left(\frac{u_0 - \phi \cdot \lambda \cdot u_1}{x_1 - x_0}\right)^{\gamma}$$

$$\text{if } \; u_0 - u_1 + \delta(x_1 - x_0) \geq 0 \;\; \text{and} \;\; \frac{x_1 - x_0}{u_0 - \phi \cdot \lambda \cdot u_1} \geq \Delta t \qquad (4.6)$$

It is obviously that driver has a high mobility is more sensitive to driver's inertia. Besides, we derive Eq. (4.7) because of $\phi \leq 1$:

$$\left(\frac{u_0 - \phi \cdot \lambda \cdot u_1}{x_1 - x_0}\right)^{\gamma} \geq \left(\frac{u_0 - \lambda \cdot u_1}{x_1 - x_0}\right)^{\gamma} \qquad (4.7)$$

In Eq. (4.7), drivers who just do lane-changing behaviors make a larger initial field than drivers who have change lane for a long time to the cars behind them. It proves the assumptions in the beginning of this chapter.

Although the meanings of parameters are identical between single and multi-lane models, some of them must be calibrated again in multi-lane models. We discuss these parameters in next chapter.

4.2 Macroscopic Model and Calibration of the Parameters

We derive the model from Eq. (4.6):

$$E_{0,In} = \frac{[u_0 - u_1 + \delta(x_1 - x_0)]}{\varepsilon}\left(\frac{u_0 - \phi \cdot \lambda \cdot u_1}{x_1 - x_0}\right)^{\gamma}$$
$$= \frac{[u_0 - u_1 + \delta(x_1 - x_0)]}{\varepsilon} \cdot \eta'(\lambda) \cdot \left(\frac{u_0 - u_1}{x_1 - x_0}\right)^{\gamma}$$
$$= -\frac{\eta'(\lambda)}{\varepsilon}\frac{(u_1 - u_0)^{\gamma+1}}{(x_1 - x_0)^{\gamma+1}}(x_1 - x_0) - \frac{\eta'(\lambda)}{\varepsilon}\delta(x_1 - x_0)\left(\frac{u_1 - u_0}{x_1 - x_0}\right)^{\gamma}$$

To obtain Eq. (4.7):

$$E_{0,In} = -\frac{\eta'(\lambda)}{\varepsilon}\frac{\partial u^{\gamma'}}{\partial x^{\gamma'}}k - \frac{\eta'(\lambda)}{\varepsilon}\delta(k)\frac{\partial u^{\gamma}}{\partial x^{\gamma}} \tag{4.7}$$

It must be noticed that Eq. (4.7) represnts that all cars just change lane for a short time. It is unreasonable to introduce Eq. (4.7) into our macroscopic mode.

Because the amount of lane-changing behaviors is expressed by density, we assume original density is *k* and shift k_c to adjacent lanes. Eq. (4.8) is derived from Eq. (4.7):

$$E_{0,In} = -\frac{\eta''(\lambda)}{\varepsilon}\frac{\partial u^{\gamma'}}{\partial x^{\gamma'}}k - \frac{\eta''(\lambda)}{\varepsilon}\delta(k)\frac{\partial u^{\gamma}}{\partial x^{\gamma}}$$
$$\eta''(\lambda) = \frac{k}{k + k_c}\eta(\lambda) + \frac{k_c}{k + k_c}\eta'(\lambda) \tag{4.8}$$

Eq. (4.8) is a kind of proportional representation. When the amount of lane-changing behaviors is larger, the shock caused by it is larger.

$\eta'(\lambda)$ is define in Eq. (4.9)

$$\eta'(\lambda)\left(\frac{u_0 - u_1}{x_1 - x_0}\right)^{\gamma} = \left(\frac{u_0 - \phi \cdot \lambda \cdot u_1}{x_1 - x_0}\right)^{\gamma}$$
$$\Rightarrow \eta'(\lambda) = \left(\frac{u_0 - \phi \cdot \lambda \cdot u_1}{u_0 - u_1}\right)^{\gamma} \tag{4.9}$$

According to the result of simulator, statistical data about $\eta'(\lambda)$ is showed in Table 4-1:

Table 4-1 Statistical data between $\eta'(\lambda)$ and mobility

Mobility	Average of $\eta'(\lambda)$	Standard deviation of $\eta'(\lambda)$
0.1	1.317	0.273
0.2	1.282	0.447
0.3	1.497	0.659
0.4	1.520	0.952

When mobility is larger, the standard deviation of $\eta'(\lambda)$ is larger.

We don't define a new equation to calculate the amount of lane-changing behaviors. So, we introduce Michalopoulos'method into this research to obtain our macroscopic model:

$$\frac{\partial q_i}{\partial x}+\frac{\partial k_i}{\partial t}=Q_i \text{ 、 } \frac{du_i}{dt}=E_{i,In}+E_{i,Ex} \text{ 、 } q_i=k_i u_i$$

$$E_{i,In}=-\frac{\eta''(\lambda)}{\varepsilon}\frac{\partial {u_i}^{\gamma'}}{\partial x^{\gamma'}}k_i-\frac{\eta''(\lambda)}{\varepsilon}\delta(k_i)\frac{\partial u_i^{\gamma}}{\partial x^{\gamma}} \quad \text{if } \frac{\partial u_i}{\partial x}+\delta'(k_i)\geq 0 \text{ and } -\eta''(\lambda)\frac{\partial u_i}{\partial x}\leq\frac{1}{\Delta}$$

$$E_{i,In}=-E_{i,Ex}-u_i \qquad \text{if } \frac{\partial u_i}{\partial x}+\delta'(k_i)\geq 0 \text{ and } -\eta''(\lambda)\frac{\partial u_i}{\partial x}\leq\frac{1}{\Delta}$$

$$E_{\mathrm{i,In}}=0 \qquad \text{if } \frac{\partial u_i}{\partial x}+\delta'(k_i)<0$$

$$E_{i,Ex}=\frac{u_e-u_i}{T} \text{ 、 } \delta'(k_i)=u_f\cdot k_i-2/\Delta \text{ 、 } u_e=u_f\, exp(\frac{k_i}{k_j})^{-0.5} \text{ 、 } \gamma'=1+\gamma=2+10\lambda$$

$$\eta''(\lambda)=\frac{k_i}{k_i+k_{i,c}}\eta(\lambda)+\frac{k_{i,c}}{k_i+k_{i,c}}\eta'(\lambda) \quad \text{、}$$

$$Q_i=\alpha_{i,i+1}\{[k_{i+1}(x,t-\Delta t)-k_i(x,t-\Delta t)]-(k_{(i+1)0}-k_{i0})\}+$$
$$\alpha_{i,i-1}\{[k_{i-1}(x,t-\Delta t)-k_i(x,t-\Delta t)]-(k_{(i-1)0}-k_{i0})\}$$

$$k_{i,c} = {\alpha_{i,i+1}}/{u_{i+1}(x,t-\Delta t)}\{[k_{i+1}(x,t-\Delta t)-k_i(x,t-\Delta t)]-(k_{(i+1)0}-k_{i0})\}+$$
$${\alpha_{i,i-1}}/{u_{i-1}(x,t-\Delta t)}\{[k_{i-1}(x,t-\Delta t)-k_i(x,t-\Delta t)]-(k_{(i-1)0}-k_{i0})\}$$

$$\alpha_{i,i\pm1}=\begin{cases}0 & if \quad |k_i(x,t-\Delta t)-k_{i\pm1}(x,t-\Delta t)|<k_A\\ \dfrac{\alpha_{max}}{k_0-k_A}|k_i(x,t-\Delta t)-k_{i\pm1}(x,t-\Delta t)|-k_A & if \quad |k_i(x,t-\Delta t)-k_{i\pm1}(x,t-\Delta t)|\geq k_A\end{cases}$$

(4.10)

In Eq. (4.10), *i* denotes the number of car. Eq. (3.10) is the models of middle lane. If someone wants to describe the inside lane, he must adjust $i\pm1$ to *i*+1. If someone wants to describe the outside lane, he must adjust $i\pm1$ to *i*-1.

CHAPTER 5
Contribution and Future Works

5.1 Contribution

We derive a new macroscopic traffic flow model based on microscopic one. It makes all variables and parameters having physic meanings. If physic meanings exit, field data can help us to calibrate the parameters conveniently. Variables in the model can also be adjusted to fit different condition easily.

We introduce traffic fields and mobility into the new model. The traffic fields represent the power that push cars to accelerate or decelerate. Dividing the fields into the internal field and the external field can simplify the movements of cars. Different magnitudes of mobility can be applied to describe different driving behaviors in the same road (Drivers in inside lane must have different mobility from in outside lane).

There is no backward flow in this new traffic flow model because of the definitions about thresholds. For example, we have three kinks of the internal fields in different situations.

5.2 Future Works

1. We don't verify the fitness of equilibrium velocity. It should be calibrate according to field data.
2. Mobility should not be the only factor to affect ε. Maybe some other factors are neglected when we design the models.
3. The .aAmount of lane-changing behaviors is still calculated from past methods. It should be designed according to the field data.
4. We don't discuss the rationality about numerical simulation in this research. It could be verified through a suitable finite difference method.
5. Two-dimension model is needed to analyze the behaviors of motorcycle. We define the meanings of the fields. The meaning of energy in traffic should

be defined in future work. Energy could be the threshold of lane-changing behaviors.

6. Mixed flow is the final work to describe real behaviors of vehicles.

References

1. Baker, R.G., "A Model of Traffic Dispersion from a Congested Road." *Transportation Research Part B* **15**, 319-327 (1981).
2. Baker, R.G.V., "On the Kinematics and Quantum Dynamics of Traffic Flow." *Transportation Research Part B* **17B**, 55-66 (1983).
3. Bando, H., Hasebe, k., Nakayama, A., Shibata, A., and Sugiyama, Y. A , "Dynamic Model of Traffic Congestion and Numerical Simulation." *Physical Review E* **51**, 1035-1042.
4. Benekohal, R. F., Treiterer, J., "CARSIM. CAR-Following Model for Simulation of Traffic in Normal and Stop-and-Go Conditions." *Transportation Research Record*, 99-111 (1988).
5. Chowdhury, D., Wolf, D. E., and Schreckenberg, M., "Particle Hopping Models for Two-Lane Traffic with Two Kinds of Vehicles: Effect of Lane-Changing Rules." *Physica A* **235**, 417-439 (1997).
6. Chronopoulos, A.T., Johnston, C. M., "A Real-Time Traffic Simulation System." *IEEE Transactions on Vehiclar Technology* **47**, 321-331 (1998).
7. Daganzo, C.F., "The Cell Transmission Model: A Dynamic Representation of Highway Traffic Consistent with the Hydrodynamic Theory." *Transportation Research Part B* **28**, 269-287 (1994).
8. Daganzo, C.F., "A Finite Difference Approximation of the Kinematic Wave Model of Traffic Flow." *Transportation Research Part B* **29**, 261-276 (1995).
9. Daganzo, C.F., "A Continuum Of Traffic Dynamics For Freeways With Special Lanes." *Transportation Research Part B* **31**, 83-102 (1997).
10. Del Castillo, J.M., Pintado, P., and Benitez, F. G., "The Reaction Time of Drivers And The Stability of Traffic Flow." *Transportation Research Part B* **28**, 35-60 (1994).
11. Del Castillo, J.M., Benitez, F. G., "On the Functional Form of the Speed-Density Relationship-I: General Theory." *Transportation Research Part B* **29B**, 373-389 (1995).
12. Del Castillo, J.M., Benitez, F. G., "On the Functional Form of the Speed-Density

Relationship-II: Empirical Investigation." *Transportation Research Part B* **29**, 391-406 (1995).

13. Duke, S., May. A , "Statistical Analysis of Speed-Density Hypotheses." *Transportation Research Board*, 154 (1967).
14. Gazis, D., Knapp, C., "On- line estimation of traffic densities from time- series of flow and speed data." *Transportation Science* **5**, 283-301 (1971).
15. Gazis, D.C., Herman, R., and Potts, R. B., "Car-Following Theory of Steady State Flow." *Operations Research* **7**, 499-505 (1959).
16. Gazis, D.C., Herman, R., and Rothery, R. W., "Non-Linear Follow-the-Leader Models of Traffic Flow." *Operations Research* **9**, 545-567 (1961).
17. Gerlough, D.L., "Simulation of Freeway Traffic by an Electronic Computer." *Proceedings of 35th Annual Meeting of Highway Research Board* (1956).
18. Gipps, P.G., "A Behavioral Car-Following Model for Computer Simulation." *Transportation Research Part B* **15**, 105-111 (1981).
19. Greenberg, H., "An Analysis of Traffic Flow." *Operations Research* **7**, 78-85 (1959).
20. Greenshields, B.D., "A study in High Way Capacity." *Highway Research Board, Proceedings* **14**, 458 (1935).
21. Hanebutte, U., Doss, E., Ewing, T., and Tentner, A., "Simulation of vehicle traffic on an automated highway system." *Mathematical and Computer Modelling* **27**, 129 (1998).
22. Hattori, Y., Hashimoto, T., and Inoue, S., "A Study for the Traffic Flow Control Considering Capacity of the Road by Cellular Automation Method." *IEEE SMC'99 Conference Proceedings* **4**, 569-573 (1999).
23. Jiang, R., Wu, Q. S., Zhu, Z. J. "A new continuum model for traffic flow and numerical tests." *Transportation Reasearch Part B* **36**, 405 - 419 (2002).
24. Jin, W., Zheng, Y., and Li, J., "Microscopic Simulation of Traffic Flow at Signalized Intersection Based on Cellular Automata." *Proceedings of IEEE International Vehicle Electronics Conference* **1**, 106-109 (1999).
25. Khan, S., Maini, P., and Thanasupsin, K., "Car-following and Collision Constraint Models for Uninterrupted Traffic: Reexamination Using High-Precision Global

Positioning System Data." *Transportation Research Record*, 37-46 (2000).

26. Leutzbach, W., "Introduction to The Theory of Traffic Flow." *Springer-Verlag* (1988).
27. Lighthill, M.J., Whitham, G. B., "On Kinematics Waves II. A Theory of Traffic Flow on Long Crowded Road." *London, Proceedings Royal Society*, 317-345 (1955).
28. Makigami, Y., Newell, G. F. ,and Rothery R., "Three-Dimensional Representation of Traffic Flow." *Transportation Science* **5**, 302-313 (1971).
29. May, A.D., *Traffic Flow Fundamentals*, (Prentice Hall, 1990).
30. Michalopoulos, P., Beskos, D., and Yamauchi, Y., "Multilane Traffic Flow Dynamics: Some Macroscopic Consideration." *Transportation Research Part B* **18**, 377-393 (1984).
31. Michalopoulos, P.G., and Pisharody, V., "Plaoon Dynamics on Signal Controlled Arterial." *Transportation Science* **14**, 365-396 (1980).
32. Michalopoulos, P.G., Stephanopoulos, G., and Pisharody, V. B., "Modeling of Traffic Flow at Signalized Links." *Transportation Science* **14**, 9-41 (1980).
33. Michalopoulos, P.G., Stephanopoulos, G., and Stephanopoulos, G., "An Application of Shock Wave Theory to Traffic Signal Control." *Transportation Research Part B* **15**, 35-51 (1981).
34. Michalopoulos, P.G., Yi, P., and Lyrintzis, A. D., "Continuum Modelling of Traffic Dynamics for Congested Freeways." *Transportation Research Part B* **27**, 315-352 (1993).
35. Nagatani, T., "Effect of Car Acceleration on Traffic Flow in 1D Stochastic CA Model." *Physica A* **223**, 137-148 (1996).
36. Nagel, K., "Partical Hopping Models and Traffic Flow Theory." *Physical Review E* **53**, 4655-4672 (1996).
37. Nagel, K., "A Cellular Automaton Model for Freeway Traffic." *Journal of Physics I* **2**, 2221-2229 (1992).
38. Newell, G. F., "A Simplified Theory of Kinematic Waves in Highway Traffic, Part 1: General Theory." *Transportation Research Part B* **27**, 281-287 (1993).
39. Newell, G. F., "A Simplified Theory of Kinematic Waves in Highway Traffic, Part II:Queueing at Freeway Bottlenecks." *Transportation Research Part B* **27**, 289-303

(1993).

40. Newell, G. F., "A Simplified Theory Of Kinematic Waves In Highway Traffic, Part III: Multi-Destination Flows." *Transportation Research Part B* **27**, 305-313 (1993).
41. Olcott, E.S., "The Influence of Vehicular Speed and Spacing on Tunnel Capacity." *Operations Research* **3**, 147-167 (1955).
42. Papageorgiou, M., Blosseville, J. M., and Had-Salem, H., "Macroscopic Modelling of Traffic Flow on the Boulevard Peripherique in Paris." *Transportation Research Part B* **16**, 125-142 (1982).
43. Payne, H.J., "Models of Freeway Traffic and Control." *Math. Models Publ. Sys. Simul. Council Proc.* **28**, 51-61 (1971).
44. Pesheva, N.C., Daneva, D. P., and Brankov, J. G., "Self-Organized Criticality in 1D Stochastic Traffic Flow Model." *Reports on Mathematical Physics* **40**, 509-520 (1997).
45. Phillips, W.F., "Kinetic Model for Traffic Flow." *National Technical Information Service, Springfield* (1977).
46. Pipes, L.A., "An Operational Analysis of Traffic Dynamics." *Journal of Applied Physics* **24**, 274-287 (1953).
47. Reuschel, A., "Vehicle Movements in a Platoon." *Oesterreichisches Ingenieur-Archir* **4**, 193-215 (1950).
48. Reuschel, A., "Vehicle Movements in a Platoon with Uniform Acceleration or Deceleration of the Lead Vehicle." *Zeitschrift des Oesterreichischen Ingenieur-und Architeken-Vereines*, 56-62 and 73-77 (1950).
49. Richards, P.I., "Shock Waves on the Highway." *Operation Research* **4**, 42-51 (1956).
50. Ricket, M., Nagel, k., Schreckenberg, M., and Latour, A., "Two Lane Traffic Simulations Using Cellular Automation." *Physica A* **231**, 534-550 (1996).
51. Ross, P., “Traffic Dynamics.” *Transportation Research Part B* , 421-435(1988)
52. Vaughan, R. J., “The Distribution of Traffic Volumes.” *Transportation Science* **4**, 97-110 (1970)
53. Widemann, R., “Simulation de Stranssenverkehrsflusses.” *Schriftenreihe des Instituts fur Verkehrswesen* (1974)

54. 羅仕京,“車流動力模式之構建與模擬 — 以波茲曼輸運方程為基礎”,國立交通大學, 博士論文, 民國 91 年.
55. 林貴億, “平行模擬車流波茲曼方程式之研究”, 國立交通大學, 碩士論文, 民國 92 年.
56. 林其蔚,“動態車流模擬與動態交通路網模式構建之研究”, 國立交通大學, 碩士論文, 民國 91 年.